NASA CR-152212

INVESTIGATION OF A LASER DOPPLER VELOCIMETER SYSTEM TO MEASURE THE FLOW FIELD AROUND A LARGE SCALE V/STOL AIRCRAFT IN GROUND EFFECT

By

Andrew D. Zalay
Melvin R. Brashears
Archie J. Jordan
Kenneth R. Shrider
Carl D. Vought

May 1979

Distribution of this report is provided in the interest of information exchange. Responsibility for the contents resides in the author or organization that prepared it.

REPRODUCED BY
NATIONAL TECHNICAL INFORMATION SERVICE
US DEPARTMENT OF COMMERCE
SPRINGFIELD, VA 22161

Prepared under Contract No. NAS2-8959
by Lockheed Missiles & Space Company, Inc.
Huntsville, Alabama

for

AMES RESEARCH CENTER

NATIONAL AERONAUTICS AND SPACE ADMINISTRATION

(NASA-CR-152212) INVESTIGATION OF A LASER DOPPLER VELOCIMETER SYSTEM TO MEASURE THE FLOW FIELD AROUND A LARGE SCALE V/STOL AIRCRAFT IN GROUND EFFECT (Lockheed Missiles and Space Co.) 76 p HC E04/MF A01 CSCL 14B G3/35 N79-26374 Unclas 28378

11

1. Report No	2 Government Accession No	3 Recipient's Catalog No
NASA CR-152212		

4 Title and Subtitle	5 Report Date
INVESTIGATION OF A LASER DOPPLER VELOCIMETER SYSTEM TO MEASURE THE FLOW FIELD OF A HOVERING V/STOL AIRCRAFT	October 1978
	6 Performing Organization Code
7 Author(s) Andrew D Zalay, Melvin R. Brashears, Archie J. Jordan, Kenneth R. Shrider and Carl D. Vought	8 Performing Organization Report No LMSC-HREC TR D568986
9 Performing Organization Name and Address Lockheed Missiles & Space Company, Inc. Huntsville Research & Engineering Center Huntsville, Alabama 35807	10 Work Unit No
	11 Contract or Grant No NAS2-9859
12 Sponsoring Agency Name and Address National Aeronautics and Space Administration Ames Research Center Moffett Field, California 94035	13 Type of Report and Period Covered Contractor Report
	14 Sponsoring Agency Code

15 Supplementary Notes

16 Abstract

An experimental research program for measuring the flow field around a hovering 70 percent scale vertical takeoff and landing (V/STOL) aircraft model is described. The velocity measurements were conducted with a ground-based laser Doppler velocimeter The remote sensing instrumentation, experimental tests, and the results of the velocity surveys are discussed The distribution of vertical velocity in the fan jet and fountain, the radial velocity in the wall jet and the horizontal velocity along the aircraft underside are presented for different engine rpms and aircraft heights above ground.

The report shows that it is feasible to use a mobile laser Doppler velocimeter to measure the flow field generated by a large-scale V/STOL aircraft operating in ground effect.

17 Key Words (Suggested by Author(s))		18 Distribution Statement
V/STOL Aircraft	Static Hover Tests	Unclassified-Unlimited
Doppler Velocimeter	Reingestion	STAR Category - 35
Jets	Recirculation	
Infrared Laser System	Velocity Footprint	

19 Security Classif. (of this report)	20 Security Classif (of this page)	21 No of Pages	22 Price*
Unclassified	Unclassified		

* For sale by the National Technical Information Service, Springfield, Virginia 22161

NASA-C-168 (Rev 10-75)

FOREWORD

This report summarizes work performed by Lockheed Missiles & Space Company, Inc., Huntsville Research & Engineering Center, Huntsville, Ala., under Contract NAS2-9859 for NASA-Ames Research Center. The NASA-Ames technical monitor was Mr. Bruno Gambucci.

The authors gratefully express their appreciation to Mr. Gambucci and to Robert Weinraub of the Advanced Aircraft Design Section of Naval Air Systems Command Headquarters for their help and advice during the study. The authors also thank Donald Esker and Ernest Schuster of McDonnel Aircraft Company for providing pressure and temperature measurements from the test of the large-scale aircraft.

Neither the United States Government nor Lockheed Missiles & Space Company, Inc., endorse products or manufacturers. Trade or manufacturers' names appear in the report because they are considered essential to the object of the report.

Preceding page blank

CONTENTS

Section		Page
	FOREWORD	iii
	LIST OF SYMBOLS	vii
1	INTRODUCTION	1
2	INSTRUMENTATION	5
	2.1 Laser Doppler Velocimeter System	5
	2.2 Data Processing	12
3	DESCRIPTION OF EXPERIMENTAL TESTS	26
	3.1 Test Program	26
	3.2 Operation of the Laser Doppler Velocimeter	26
4	RESULTS OF LASER DOPPLER VELOCIMETER MEASUREMENTS	34
	4.1 Characteristic Velocity Signature	34
	4.2 Wall Jet Decay	42
	4.3 Fan Jet	42
	4.4 Fountain	47
	4.5 Flow Along Fuselage	50
5	CONCLUSIONS AND RECOMMENDATIONS	53
	REFERENCES	55
Appendixes		
A	Description of Laser Doppler Velocimeter System	A-1
B	Summary of Velocity Measurements Obtained with Laser Doppler Velocimeter	B-1

LIST OF TABLES

Table		
1	Test Conditions for Flowfield Surveys with LDV System	27
2	Scan Patterns Utilized During V/STOL Test	31

LIST OF FIGURES

Figure		Page
1	Flow Field About a V/STOL Aircraft in Ground Effect	1
2	Lockheed LDV System Deployed at NASA-Ames Research Center for V/STOL Flowfield Surveys	6
3	Sketch of Remote Mirror Assembly for Vertical V/STOL Flowfield Measurements	7
4	Photograph of Laser Doppler Velocimeter Van and Mobile Computer Facility Trailer	8
5	Interior View of Laser Doppler Velocimeter Van Depicting Display and Scanner Controls in First Rack, Computer in Second Rack, Digital Tape Unit Aft and Optics Package on Right	9
6	Interior View of Mobile Computer Facility Trailer Showing PDP 11/34 Computer	10
7	Typical Output from LDV System	14
8	Sample Output from IVPPRZ Progrsm Showing Survey of Wall Jet from L/C Fan Engine in Nose of Aircraft	16
9	Sample Output from VTAVQQ Program Showing Distribution of Horizontal Velocity in Wall Jet from Nose Fan	18
10	Geometry for Remote Mirror and Traverse Assembly Incorporated into the PLOT Program	20
11	Sample Output from ANDYYY Program Showing Distribution of Maximum Vertical Velocity Between Aircraft and Ground from Nose Fan Along Aircraft Centerline	21
12	Sample Output from ANDKEN Program Showing Distribution of Horizontal Velocity in Wall Jet from Nose Fan	23
13	Sample Output from ANDTRN Program Showing Distribution of Vertical Velocity Below Nose Fan Along Aircraft Centerline	25
14	Deployment of LDV System at NASA-Ames	30
15	Sketch of Test to Investigate Influence of Temperature and Turbulence Gradients on Return Signal	33
16	Signature from LDV During Survey of Wall Jet of V/STOL Aircraft	35
17	Magnitude of the Line-of-Sight Velocity as a Function of Range for Scans Through the Wall Jet of the Nose Fan at 3600 rpm for Aircraft Height of 1.5 m	37
18	Magnitude of the Backscatter Intensity, ISUM, as a Function of Range for Scans Through the Wall Jet of the Nose Fan, Aircraft Height 1.5 m, Nose Fan at 3600 rpm	

Figure		Page
19	Number of Data Acceptables, N, as a Function of Range for Range Scans Through the Wall Jet of the Nose Fan for Aircraft Height 1.5 m, Nose Fan at 3600 rpm	40
20	Comparison of Maximum Line-of-Sight Velocities Computed for Wall Jet Near Ground from Nose Fan	41
21	Distribution of Peak Velocities Near Ground Below Nose Fan	43
22	Maximum Velocity in Wall Jet as a Function of Fan rpm	44
23	Distribution of Vertical Velocity Along Aircraft Centerline at Location of Nose Fan	45
24	Mean Vertical Velocity at Nozzle Exit of Nose Fan Measured by LDV and Pitot Probe	46
25	Distribution of Vertical Velocity Along Aircraft Centerline Near Ground for Two-Jet Fountain	48
26	Distribution of Vertical Velocity as a Function of Height Above Ground in Two-Jet Fountain	49
27	Distribution of Vertical Velocity Along Aircraft Centerline Near Ground for Two- and Three-Jet Fountain	51
28	Distribution of Horizontal Velocity Along Aircraft Centerline on Bottom of Fuselage	52

LIST OF SYMBOLS

Symbol	Description
β	angle between ground plane and focal volume of LDV (deg)
γ	angle between traverse and focal volume of LDV (deg)
θ	tilt of traverse (deg)
ρ	density of particulates (gm/m^3)
D	jet diameter (D = 1 m)
E	distance between two lift cruise fans (E = 2.6 m)
H	height above ground (m)
I_m	maximum signal intensity (V)
I_o	amplitude threshold (V)
IPV	velocity (frequency) corresponding to maximum signal intensity for integrated spectrum
ISUM	integrated backscatter intensity (V)
N	number of acceptable velocity (frequency) bins
RD	lateral distance from centerline of jet exhaust nozzle to focal volume of LDV (m)
R_T	lateral position of remote mirror along ground (m)
R_v	range of van from original of traverse mechanism (m)
RRR	distance from origin of traverse mechanism to focal volume of LDV (m)
u, v	velocity components measured in x, y coordinate system (m/sec)
V_j	mean jet exhaust velocity from nozzle measured by pressure probe (m/sec)

V_{max}	highest acceptable velocity (frequency) (m/sec)
V_o	velocity (frequency) threshold (m/sec)
V_{pk}	velocity (frequency) corresponding to maximum signal intensity
(x, y)	coordinate system referenced to traverse mechanism oriented with respect to horizon
(xx, yy)	coordinate system referenced to traverse mechanism
(x', y')	coordinate system referenced to jet exhaust nozzle
x_o	lateral distance from side window of LDV van to centerline of jet exhaust nozzle (m)
x_T	lateral distance of remote mirror from origin of traverse mechanism (m)
x_v	lateral distance of van from origin of traverse mechanism
xx_o	lateral distance of jet centerline from origin of traverse mechanism
y_o	vertical distance from ground to mirror in side window of van (m)
y_p	vertical distance of focal volume from jet exhaust nozzle (m)
y_v	vertical distance of mirror in side window of van from origin of traverse mechanism (m)
yy_o	vertical distance of jet centerline from origin of traverse mechanism

1. INTRODUCTION

NASA-Ames Research Center and the U.S. Navy are actively engaged in a program to provide technology for the design and development of future advanced vertical takeoff aircraft. Efficient high performance aircraft with a vertical or short takeoff and landing (V/STOL) capability are under study for naval and marine applications. This type of aircraft shows significant potential for extending current mission capabilities. The V/STOL aircraft also introduces unique aerodynamic design problems.

Propulsion-induced lift effects play an important role in the design of V/STOL aircraft. A complex flow field is generated by a V/STOL aircraft operating near the ground during takeoff and landing as sketched in Fig. 1.

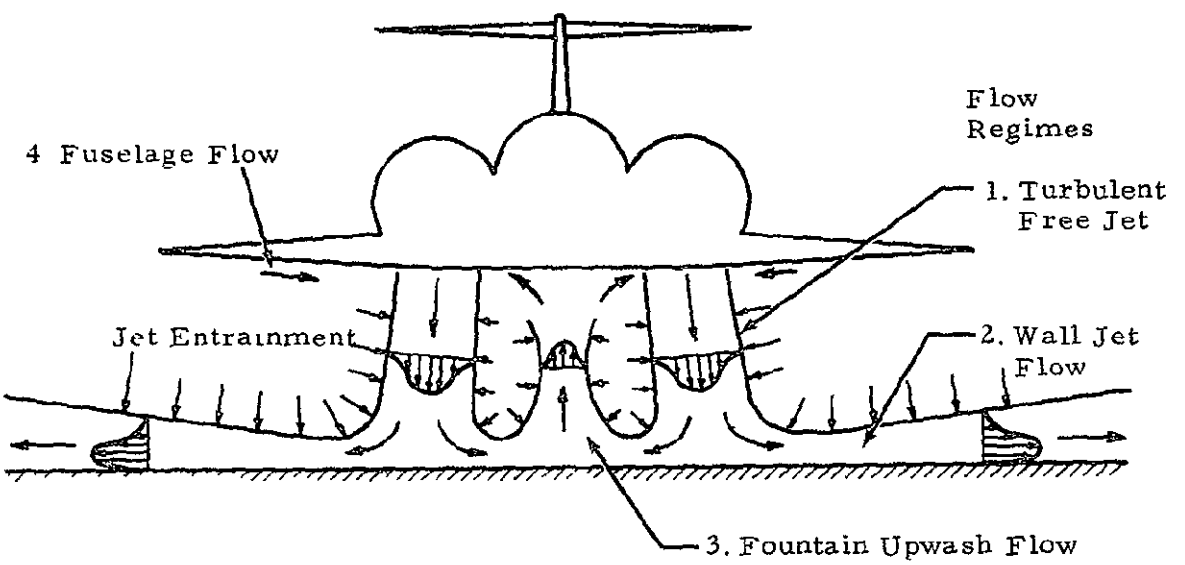

Fig. 1 - Flow Field About a V/STOL Aircraft in Ground Effect

The flow field is characterized by: (1) the turbulent free jets from the lift cruise engines; (2) the wall jet regions; (3) the fountain upwash flow region; and (4) flow along the fuselage. Entrainment of the ambient air by the turbulent free jets induces a flow of air around the aircraft. This results in a "suckdown" force on the vehicle. The turbulent jet impinges on the ground and generates a wall jet flow. A merging of the radial wall jets results in a stagnation region near the aircraft centerline. At the stagnation region, the opposing flow is turned in the vertical direction creating a hot gas fountain. Impingement of the fountain on the fuselage produces lift, heats the airframe surface and generates flow along the fuselage.

The complex flow fields of V/STOL aircraft in hover are extremely difficult to measure accurately by conventional pressure sensing devices, particularly in areas of high flow interactions. Even in the detailed design development stage of V/STOLs, gross force and moment measurements and inlet temperature data are the principal measurements obtained with only a limited knowledge of the detailed structure of the flow field. However, since the secondary flow which produces forces on the model is a strong function of the jet entrainment, a knowledge of the details of the flow field is necessary. Currently, a number of computer programs are under development for modeling the behavior of V/STOL aircraft in ground effect (Refs. 1 through 3). Each of these predictive models requires experimental measurements of the three-dimensional flow and the turbulent mixing process in the aircraft near wake.

The traditional experimental techniques for determining propulsion induced lift effects consist of: (1) measurements of the forces and moments about the aircraft center of gravity using strain gauge balances; (2) measurements of the distribution of static pressure at the surface of the aircraft or near the ground with pressure transducers; and (3) measurements of the distribution of temperature at the surface of the aircraft or near the ground with thermocouples. The balance measurements show the effect of variations in aircraft configuration and operating conditions on the induced lift. The pressure and temperature measurements provide a qualitative characterization of the external flow.

Recently, pressure and temperature measurements were carried out in the flow field of a hovering VAK-191B aircraft by a team from U.S. Navy and VFW-Fokker (Ref. 4). The measurements of aircraft footprint indicated the need for improved flow sensing techniques.

While the traditional measurement techniques show the gross effects of the jet induced flow, they do not provide sufficient information to model the complete three-dimensional flow field analytically. For example, analytic models based on a solution of the Navier-Stokes equation require specification of the turbulence field. The turbulence coefficients such as the Reynolds stresses are necessary to describe the jet entrainment and secondary flow. These turbulence parameters cannot be measured with conventional pressure transducers or temperature sensors. Because of the complexity of the flow field, new measurement techniques are necessary for providing characterization of the V/STOL flow field.

A mobile laser Doppler velocimeter (LDV) has been developed for remote sensing of atmospheric flows (Refs. 5 and 6). The LDV holds considerable promise for providing detailed surveys of the flow field of V/STOL aircraft. Recognizing the necessity for advanced flow measurement techniques, NASA-Ames Research Center supported the present study. The objective was to investigate the feasibility of a system for measuring the flow field around a hovering V/STOL aircraft. The motivating questions were: Will an LDV system function in the hot, dirty, turbulent exhaust gases emanating from a large scale V/STOL aircraft? Can the LDV be configured to measure the vertical and horizontal flow field of the aircraft operating in ground effect? Are the measurements provided by the LDV useful in the study of propulsion induced aerodynamics?

The LDV measurements were a part of a larger experimental program to determine the propulsion induced lift effects for a three-ton lift cruise subsonic V/STOL aircraft (Refs. 7 through 9). Balance measurements and temperature and static pressure surveys were obtained during simulated hover tests in an outdoor test stand facility at NASA-Ames for a 0.7 scale powered

aircraft model which are described in Ref. 8. These large scale ground hover tests afforded a unique opportunity to obtain flowfield measurements with a non-intrusive flow measuring system at the same time.

The specific objectives of the present effort were to: (1) evaluate the LDV as a possible method of measuring the flow velocities around a hovering three-fan V/STOL aircraft model; (2) obtain flow velocity measurements around a three-fan large scale V/STOL aircraft model during static tests; and (3) determine the usefulness of velocity measurements taken by the LDV in the study of ground effect of hovering V/STOL aircraft. The results of the V/STOL flowfield surveys with the mobile LDV system are described in this report including a discussion of the instrumentation, experimental tests and the results of the measurements.

2. INSTRUMENTATION

The flowfield measurements around the V/STOL aircraft were carried out by means of a laser Doppler velocimeter (LDV) system contained in a mobile van. Laser Doppler velocimetry is a proven concept for the accurate remote measurement of atmospheric flows. An LDV system senses air motion by illuminating a "sensing volume" in space with laser radiation and measuring the Doppler shift of the radiation backscattered by particulates contained in this volume. The Doppler shift of the backscattered laser energy is a direct measure of the magnitude of the velocity along the line of sight (along the laser beam) within the sensing volume. The principle of operation of the LDV system used for the flowfield measurements around the V/STOL aircraft is summarized in Appendix A. The implementation of the field-type LDV unit utilized during this investigation is discussed in this section.

2.1 LASER DOPPLER VELOCIMETER SYSTEM

The mobile LDV hardware utilized during this program is depicted in Figs. 2 through 6. The LDV van is shown deployed at NASA-Ames Research Center in Fig. 2. Details of the remote mirror assembly used for portions of the test are sketched in Fig. 3. Since the LDV is capable of measuring the magnitude of velocity along the line of sight, a remote mirror was necessary for turning the laser beam in the vertical direction for obtaining measurements of the vertical velocity. The mirror and shield assembly shown in Fig. 3 was designed to withstand the hot exhaust gases from the jet engines. A fluidic seal or air diode was incorporated into the design to minimize jet impingement on the mirror. The fluidic seal consisted of a cylinder with a series of cones inside to resist the flow. The mirror was mounted on a 3 m long traverse mechanism so that the distribution of the vertical line-of-sight velocity could be measured at different positions under the aircraft. The LDV system was scanned in range through the remote mirror to survey the flow

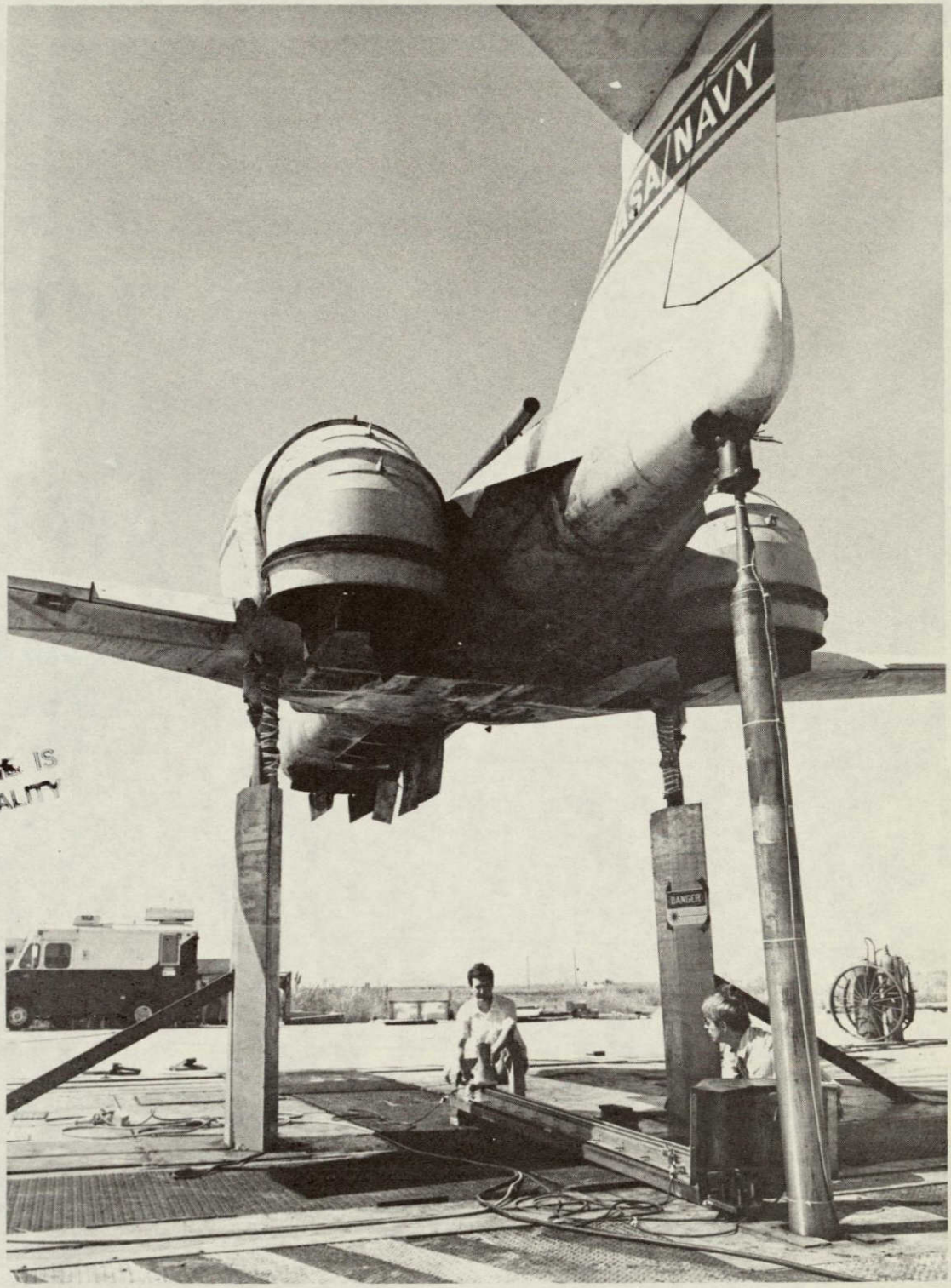

ORIGINAL PAGE IS
OF POOR QUALITY

Fig. 2 - Lockheed LDV System Deployed at NASA-Ames Research Center for V/STOL Flowfield Surveys (Note traverse mechanism and shielded mirror located below aircraft.)

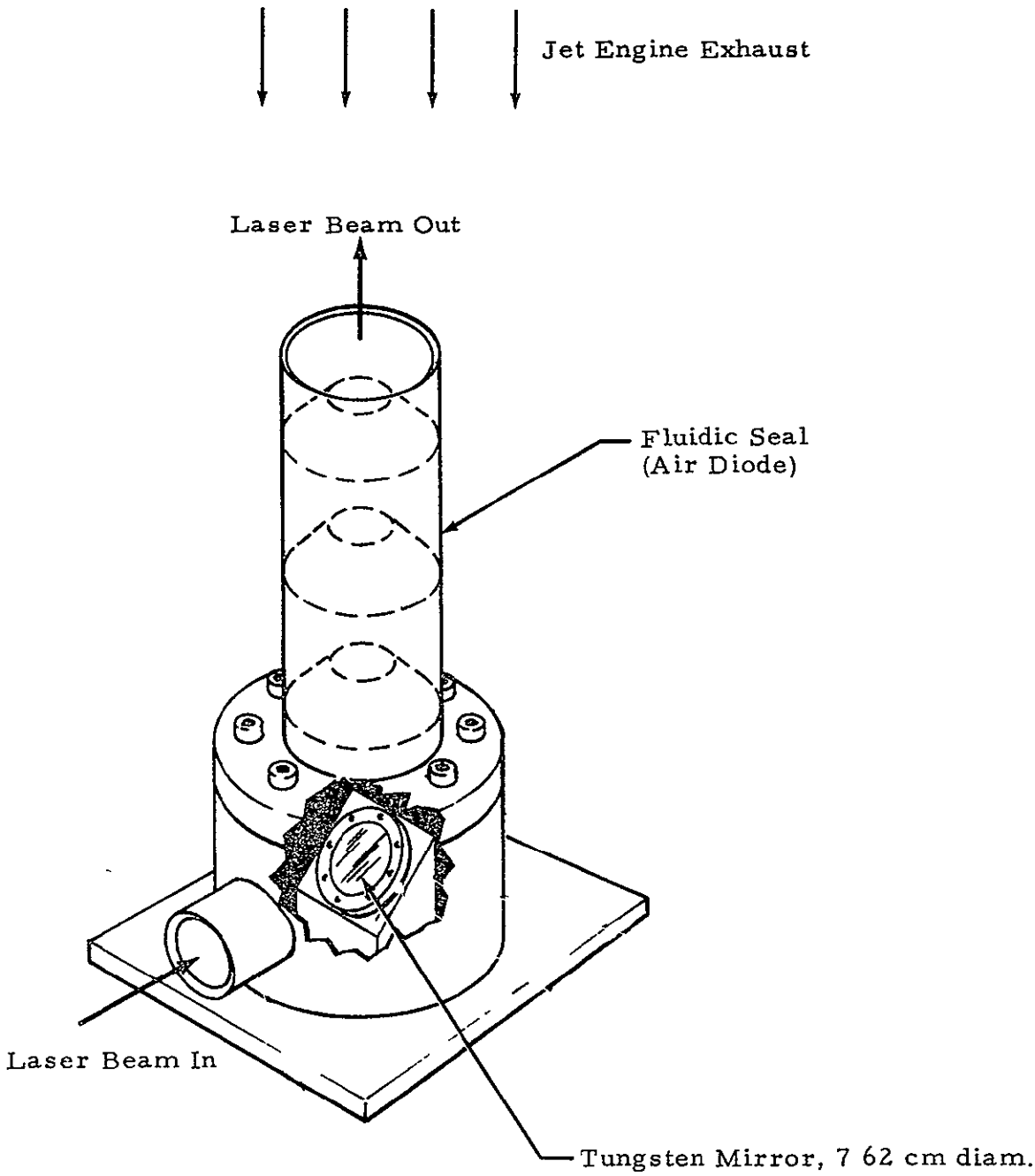

Fig. 3 - Sketch of Remote Mirror Assembly for Vertical V/STOL Flowfield Measurements

ORIGINAL PAGE IS
OF POOR QUALITY

Fig. 4 - Photograph of Laser Doppler Velocimeter Van (Right) and Mobile Computer Facility Trailer (Left)

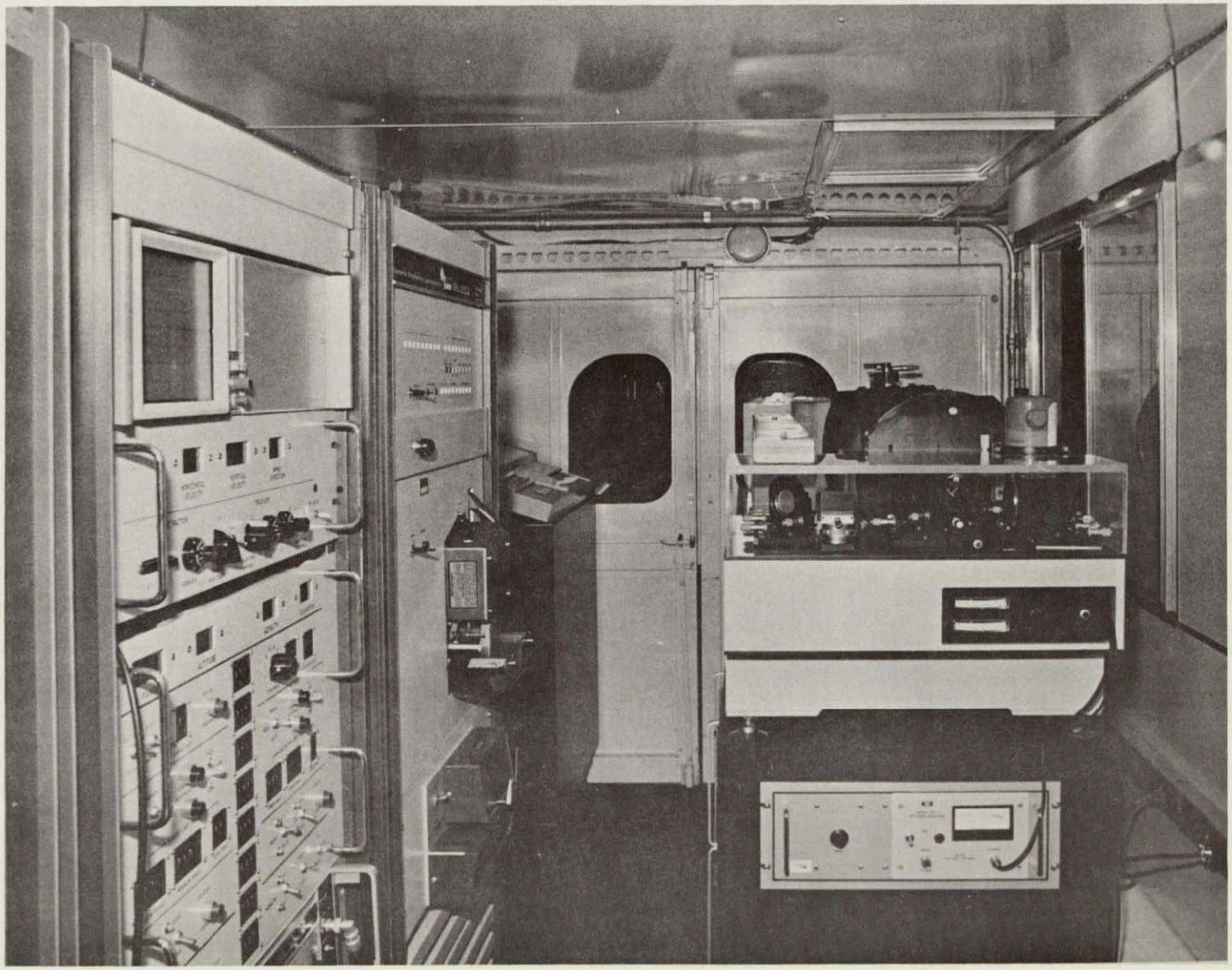

Fig. 5 - Interior View of Laser Doppler Velocimeter Van Depicting Display and Scanner Controls in First Rack, Computer in Second Rack, Digital Tape Unit Aft and Optics Package on Right

ORIGINAL PAGE IS
OF POOR QUALITY

Fig. 6 - Interior View of Mobile Computer Facility Trailer
Showing PDP 11/34 Computer

field at different vertical positions. For measurements of horizontal velocity, the remote mirror was not required and the LDV was scanned in range at different elevation angles. The measurements of the frequency and amplitude of the backscattered laser energy were processed to determine the distribution of velocity around the V/STOL aircraft.

The LDV system consisted of the LDV van, shown earlier in Fig. 2, and a trailer housing the computer equipment. A photograph of the LDV van and Mobile Computer Facility Trailer is given in Fig. 4. Interior views of the LDV van and computer trailer are given in Figs. 5 and 6, respectively.

The pertinent operating characteristics of the LDV system used in the Ames V/STOL measurement tests are summarized as follows:

Performance

1. Velocity Measurement Threshold: 1.06 m/sec
2. Velocity Range: 1.06 to 106 m/sec
3. Velocity Resolution: 1.6 m/sec

Sample Rate

1. Seventy Sample Points per sec

Spatial Resolution

1. Range Accuracy: ± 0.4 m at 24 m
2. Elevation Angle Accuracy: ± 0.25 deg

Scan Modes

1. Range Scan at Fixed Elevation and Azimuth Angle
2. Range Scan at Fixed Azimuth Variable Elevation Angle

3. Range Scan at Fixed Azimuth Angle and Discrete Elevation Angle
4. Range Scan Through Remote Mirror

The LDV operating mode during the Ames tests consisted primarily of range scans at specified azimuth and elevation angles through the side window of the LDV van. The overhead scanner with its three-dimensional scan capability was not used. The beam from the overhead scanner exited at an altitude of 3 m and could not be lowered to the ground level without hardware modifications. The static test facility at Ames was not prepared to accommodate the LDV van at an altitude such that the overhead scanner could be leveled with the test pad for the V/STOL flowfield surveys.

Since the objective of the tests was a feasibility demonstration, no hardware modifications were carried out to the LDV system. The following limitations were noted: (1) the flow direction (+ or -) along the line of sight could not be determined; (2) the sampling rate of 70 signatures per second was not sufficient to obtain measurements of the high frequency turbulence; and (3) a full three-dimensional scanning of the flow field could not be accommodated. It was recognized that the above limitations could be eliminated once the basic feasibility of the system was demonstrated. For subsequent efforts, the following hardware modifications could be implemented: (1) a translator or acousto-optic modulator (Bragg-Cell) added to the system to enable measurements of the direction of the line-of-sight velocity; (2) a surface acoustic wave (SAW) processor substituted for the spectrum analyzer to increase the sampling rate to 500 signatures per second; and (3) a ramp constructed at the site to accommodate the LDV van such that the overhead scanner would be at ground level and the existing three-dimensional scanning capabilities of the system could be utilized.

2.2 DATA PROCESSING

The output from the LDV system, consisting of the coherent backscatter intensity versus frequency from the focal volume as well as the location of the

focal volume in space, was processed to yield the velocity field in the vicinity of a V/STOL aircraft. A brief discussion of the LDV data processing system and the data processing algorithms developed for the V/STOL flow surveys are discussed in the following sections.

2.2.1 Signal Processing System

The Doppler frequency shift of the photodetector output is processed by a spectrum analyzer which provides frequency spectra (intensity of returned signal as a function of Doppler shift) at a rate of 70 signatures per second. The resolution and range of the velocities (frequencies) measured with the LDV is determined largely by the spectrum analyzer settings. During the Ames tests, the spectrum analyzer was set at 0 to 20 MHz corresponding to a velocity range of 0 to 106 m/sec. Sample runs indicated that the observed velocities of the V/STOL flow field were generally within this range. The bandwidth of the spectrum analyzer, defined as the frequency span where the signal decreased 3 dB, was set at 300 kHz corresponding to approximately 1.6 m/sec resolution in velocity.

The characteristic output signature from the LDV, the amplitude-velocity spectrum, is given in Fig. 7. The output signature shows the motion of particles within the focal volume at a given instant in time. To facilitate processing the LDV signature, velocity and amplitude thresholds were applied to the signal and the velocities (frequencies) associated with the highest intensity, V_{pk}, and highest velocity, V_{max}, above the threshold settings were extracted from the spectrum. The velocity V_{pk} is the magnitude of the line-of-sight velocity of the most intense signal. It is characteristic of the mean velocity in the focal volume. The velocity V_{max} is a measure of the maximum velocity above threshold encountered in the focal volume. It is characteristic of the maximum velocity in the focal volume. The intensity and velocity information is discretized into bins corresponding to digital values and fed into a computer for processing in real-time or in the replay mode.

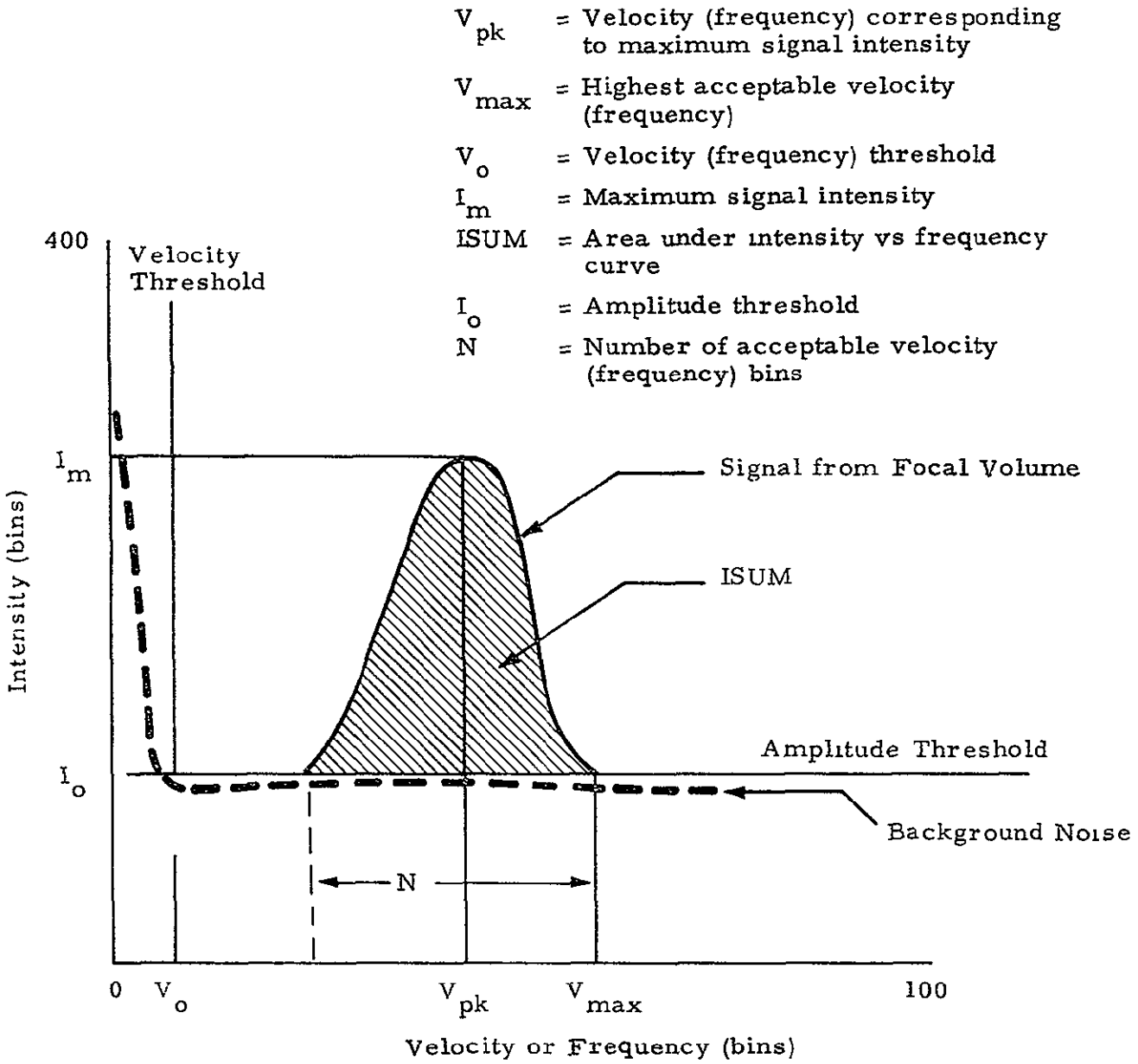

Fig. 7 - Typical Output from LDV System

2.2.2 Data Recording and Display in Real Time

The primary data gathering function is performed by a PDP 11/34 general purpose minicomputer. Data gathered by the LDV system is formatted by the computer software and stored on magnetic tape for playback and reprocessing. The DEC 9-track tape control and magnetic tape units allow digital recording of data at 800 bpi at 45 ips. The data logged by the computer include: (1) all scan volume location parameters (range, azimuth, elevation angle); (2) "mode of operation" identifier (type of scan); (3) the instantaneous line-of-sight velocity information (V_{pk}, V_{max}); (4) the Doppler spectrum peak strength (I_m); (5) spectrum intensity information (ISUM); and (6) a data quality identifier in terms of the number of data acceptable, N, the number of frequency bins from the total 100 bins which have data which meet the specified amplitude and velocity threshold criteria. When the LDV is operated using the side view window (instead of the overhead scanner) only the range of the focal volume is logged by the computer. The azimuth and elevation angles are recorded manually.

The above LDV parameters, V_{pk}, V_{max}, ISUM and N, are displayed as a function of range or time on the CRT in real time via the IVPPRZ program. A sample output from the IVPPRZ program is shown in Fig. 8. This program enables the operator to monitor the real-time data acquisition process at the site.

2.2.3 Data Processing and Display in the Replay Mode

Software is also available with the LDV system to carry out data processing and plotting in the replay mode. The data logged on 9-track tapes is replayed via the IVPPRZ program to generate plots of V_{pk}, V_{max}, ISUM or N versus range or time. The program retrieves data using the run time or file number as an input.

Analysis of the V/STOL flowfield surveys using the IVPPRZ program showed large fluctuations in the velocity attributed to high turbulence levels.

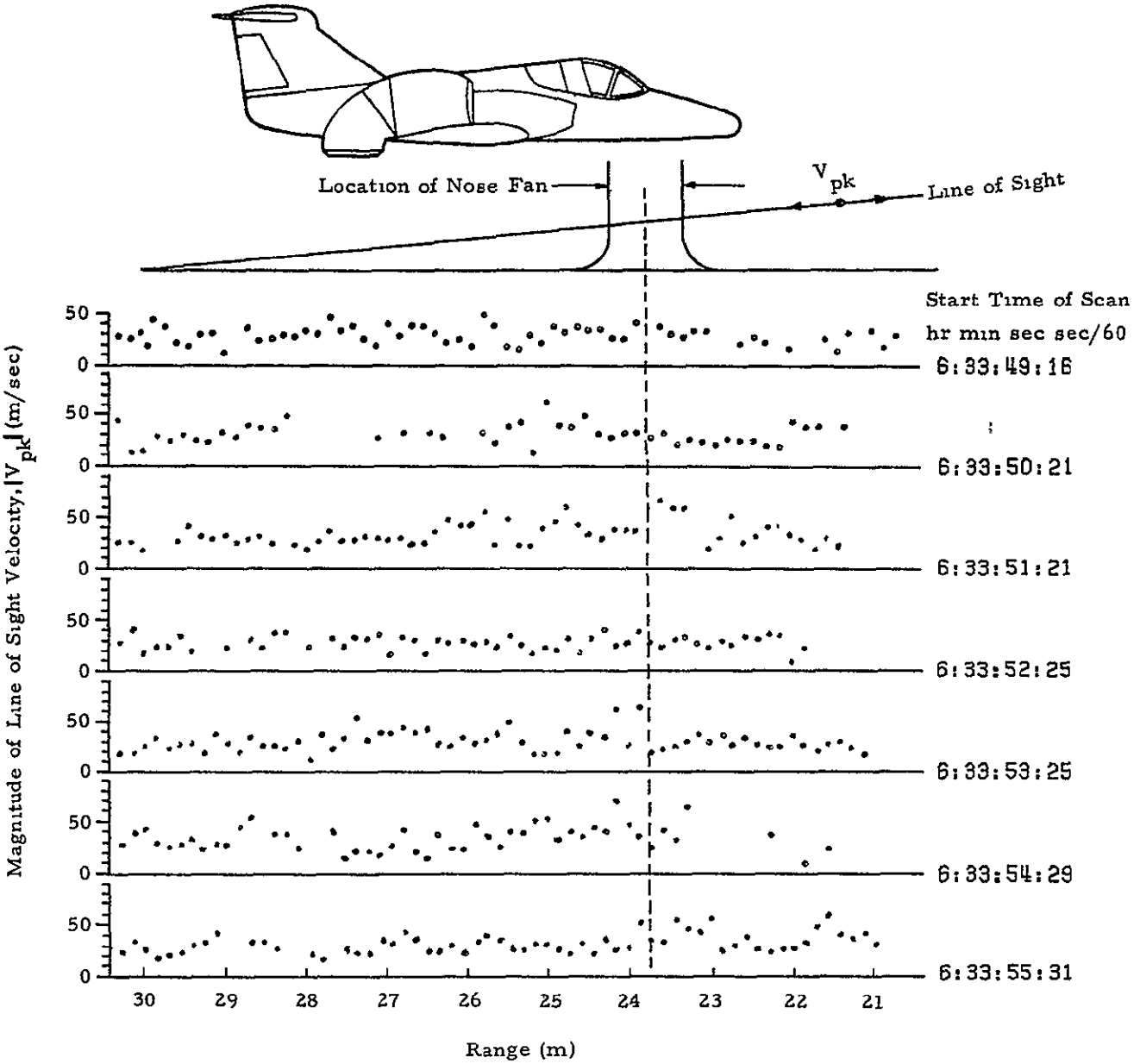

Fig. 8 - Sample Output from IVPPRZ Program Showing Survey of Wall Jet from L/C Fan Engine in Nose of Aircraft

However, it is recognized that the relatively long focal volume of the LDV in comparison to the spatial gradients in the flow field and an uneven distribution of aerosols can also contribute to fluctuations in the observed line-of-sight velocity distribution. The presence of velocity gradients (or turbulence) in the focal volume leads to a broadening of the velocity spectrum shown earlier in Fig. 7, making the identification of V_{pk} more difficult. An uneven distribution of aerosols can introduce a bias error since particles with a large cross section outside the immediate focal volume may produce sufficient backscatter intensity to override the signal from the particles within the focal volume. For these reasons, efforts were made to develop processing techniques which would minimize the scan-to-scan variations in the velocity distribution due to turbulence, poor spatial resolution and non-uniform seeding of the flow.

Essentially two different types of programs were developed for processing the sequential LDV measurements to extract the general flow trends. Both programs divide the range excursions in the horizontal and/or vertical direction into discrete bins and process sample points falling within these bins. The first type of program, illustrated by the VTAVQQ and ANDYYY codes, performs an averaging in time to determine the mean, standard deviation and range of the values sampled in each range bin. The second type of program, illustrated by the ANDKEN and TRANAV codes, performs a spectral averaging to select the velocity with the highest consistent intensity from the sampling points in each range bin. Each of these programs is discussed briefly below.

The VTAVQQ program computes and plots the following parameters as a function of range; $\overline{V}_{pk}$, $\overline{V}_{max}$, $\sigma_{V_{pk}}$, $\sigma_{V_{max}}$, max V_{max}, and the number of sample points in each range bin, N. The VTAVQQ program is useful for processing the horizontal range scan measurements to define the velocity distribution of the wall jets or flow along the aircraft fuselage. An example of the output from the VTAVQQ program is shown in Fig. 9.

For processing the vertical line-of-sight velocity distribution obtained using the remote mirror and traverse, the ANDYYY program was developed. The ANDYYY program computes the magnitude of the vertical velocity, V_{pk}

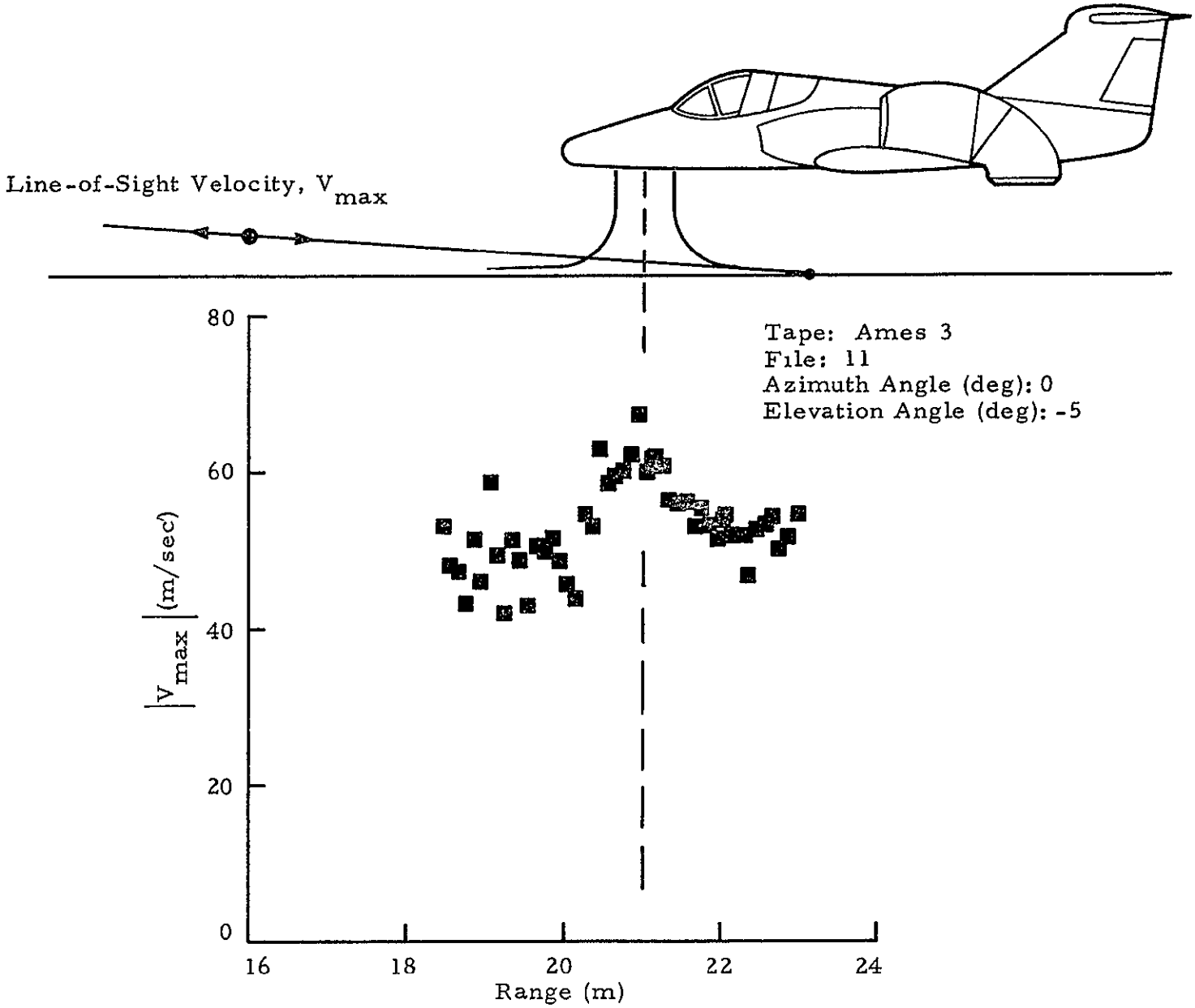

Fig. 9 - Sample Output from VTAVQQ Program Showing Distribution of Horizontal Velocity in Wall Jet from Nose Fan

or V_{max}, as a function of distance from the jet (or fountain) centerline. The input measurements consist of the range of the LDV focal volume and the position of the remote mirror along the traverse as a function of time. The initial parameters include the position of the traverse mechanism and the position of the jet (or fountain) centerline. The geometry for the remote mirror and traverse assembly incorporated into the program is shown in Fig. 10.

A sample output from the ANDYYY program is shown in Fig. 11 for a traverse through the jet exhaust from the front L/C fan engine. Since the program does not consider spatial variations in the vertical direction, the velocity profile in Fig. 11 shows the maximum vertical velocity occurring between the aircraft and the ground plane. The ANDYYY program carries out the following steps: (1) divides the total traverse excursion into approximately 100 traverse bins; (2) stores each velocity measurement (i.e., the value of V_{pk}) into a traverse bin whenever the location of the LDV sensing volume lies between the remote mirror and the underside of the aircraft; (3) after a run is completed (typical duration 60 sec) it computes the mean and the highest value of the magnitude of the line-of-sight velocity in each range bin; and (4) plots the selected velocities versus lateral distance from the jet (or fountain) centerline. The output from the ANDYYY program is the horizontal distribution of the vertical velocity between the aircraft underside and the ground. The ANDYYY program is useful for identifying the distribution of maximum vertical velocity occurring below the nose fan and fountain. The maximum vertical velocity occurs at the exit of the nose fan and near the ground for the two-jet fountain.

Comparing the raw velocity measurements shown in Fig. 8 with the averaged measurements shown in Fig. 9, it is seen that the general flow trends are identified more easily from the averaged data. However, significant scatter still exists in the averaged data as illustrated by Fig. 11. This scatter could be reduced if more sampling points were available for averaging. Since the length of the records was fixed at approximately 60 sec (corresponding to 4200 sampling points) a different processing technique was sought to further reduce the spurious variations in the velocity field. Two programs, ANDKEN and TRANAV, were developed using a spectral averaging technique.

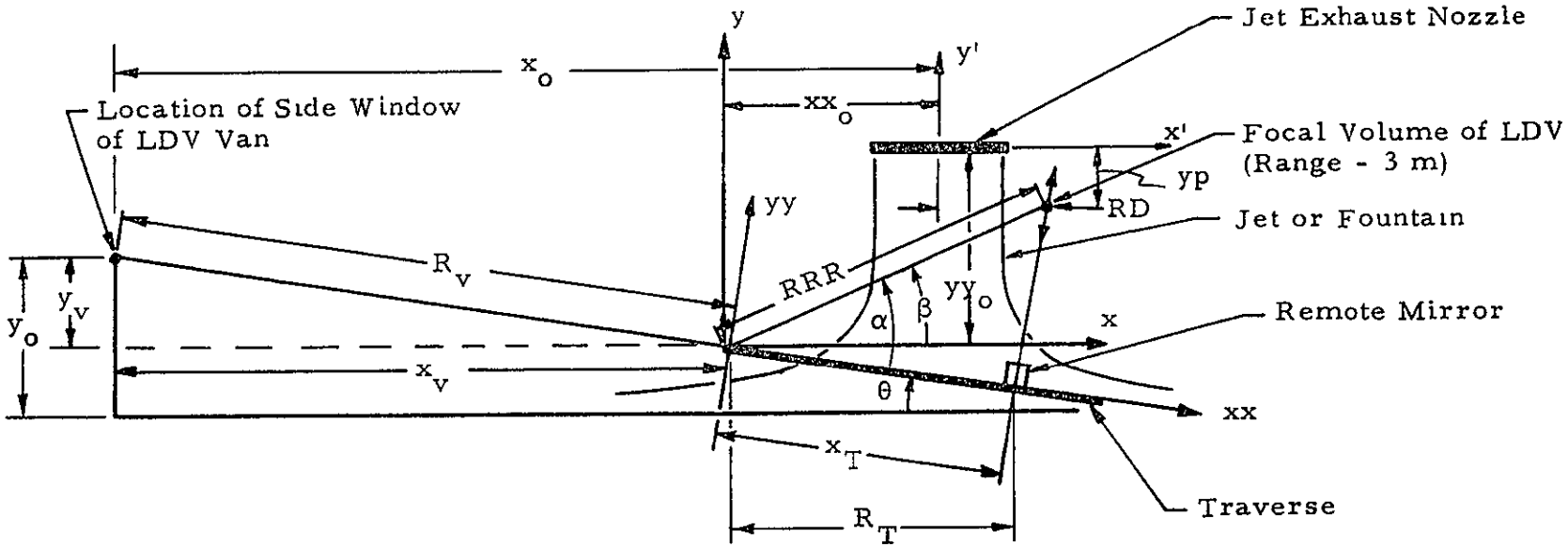

Input: Range of focal volume center from van (i e., range setting in LDV van)

θ = Tilt of traverse = $\tan^{-1}(y_v/x_v)$

x_T = Lateral distance of remote mirror from origin of traverse mechanism

x_v = Lateral distance of van from origin of traverse mechanism

y_v = Vertical distance of mirror inside window of van from origin of traverse mechanism

R_v = Range of van from origin of traverse mechanism; $R_v = \sqrt{x_v^2 + y_v^2}$

xx_o = Lateral distance of jet centerline from origin of traverse mechanism

yy_o = Vertical distance of jet centerline from origin of traverse mechanism

Output: RD = Lateral distance of focal volume from jet centerline

y_p = Vertical distance of focal volume from jet exhaust nozzle

Coordinates: (x', y') Coordinate system referenced to jet exhaust nozzle

(xx, yy) Coordinate system referenced to traverse mechanism

(x,y) Coordinate system referenced to traverse mechanism oriented with respect to horizon

Fig. 10 - Geometry for Remote Mirror and Traverse Assembly Incorporated into the PLOT Program

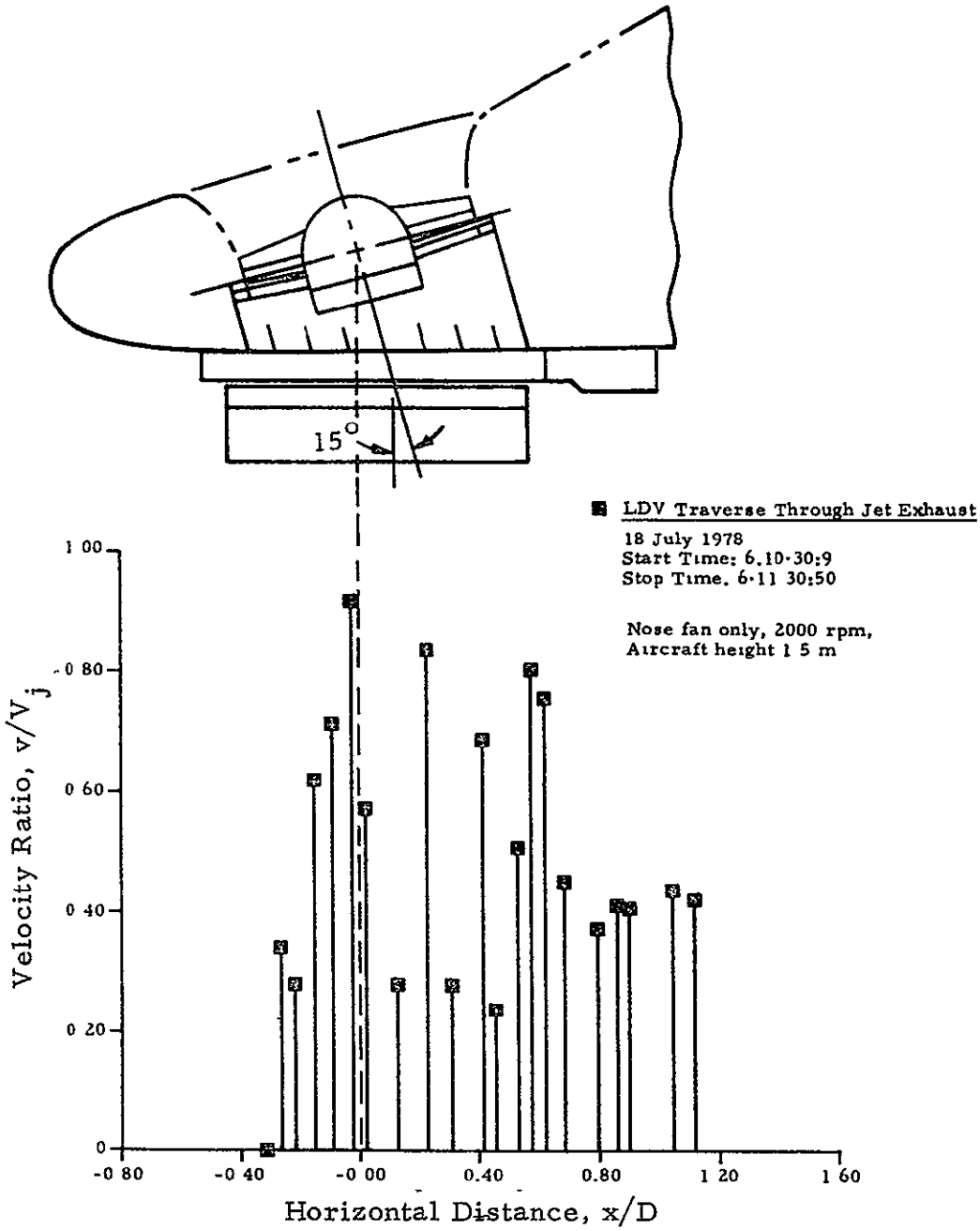

Fig. 11 - Sample Output from ANDYYY Program Showing Distribution of Maximum Vertical Velocity Between Aircraft and Ground from Nose Fan Along Aircraft Centerline

The ANDKEN program generates plots of the velocity from the integrated velocity spectrum, IPV, versus range. The program carries out the following operations: (1) the total range excursion is divided into 40 range increments; (2) for each range bin a two-dimensional array of signal intensity (100 bins) versus velocity (100 bins) is established; (3) the contribution at each range bin from each sampling point is stored in the composite intensity, $\sum_{i=1}^{i=n} I_i$ versus velocity array (n is typically 5 to 20); (4) after a run is completed (typical duration 60 sec) the velocity bin, IPV, corresponding to the highest composite intensity is selected for each range bin; and (5) the selected IPV values, representative of the spectral average of the velocity, are plotted as a function of range.

Since the highest composite intensity is associated with the velocity at the center of the LDV focal volume, the ANDKEN program eliminates variations in the observed velocity field due to nonuniform seeding or spatial resolution problems. A sample output from the ANDKEN program is shown in Fig. 12 for a range scan through the wall jet from the nose fan. A line is faired through the maximum IPV values to indicate the characteristic velocities in the flow. The scattered low IPV values are associated with range bins with insufficient number of data points for accurate definition of the flow. In comparison to the averaging technique illustrated earlier in Fig. 9, the spectral averaging technique shown in Fig. 12 provides more details of the flow field. The double peak signature in Fig. 12 is indicative of the stagnation flow near the jet centerline. The single peak signature in Fig. 9 suggests that the effective range resolution available with this averaging technique is large compared to the dimensions of the flow.

While the ANDKEN program handles horizontal range scans, a second spectral averaging code, ANDTRN was developed to process both horizontal and vertical range scans. The ANDTRN program incorporates the geometry for the remote mirror and traverse assembly illustrated earlier in Fig. 10. The program computes the spectral average of the velocity, IPV, for a rectangular 10 x 10 grid according to the technique discussed earlier. A sample

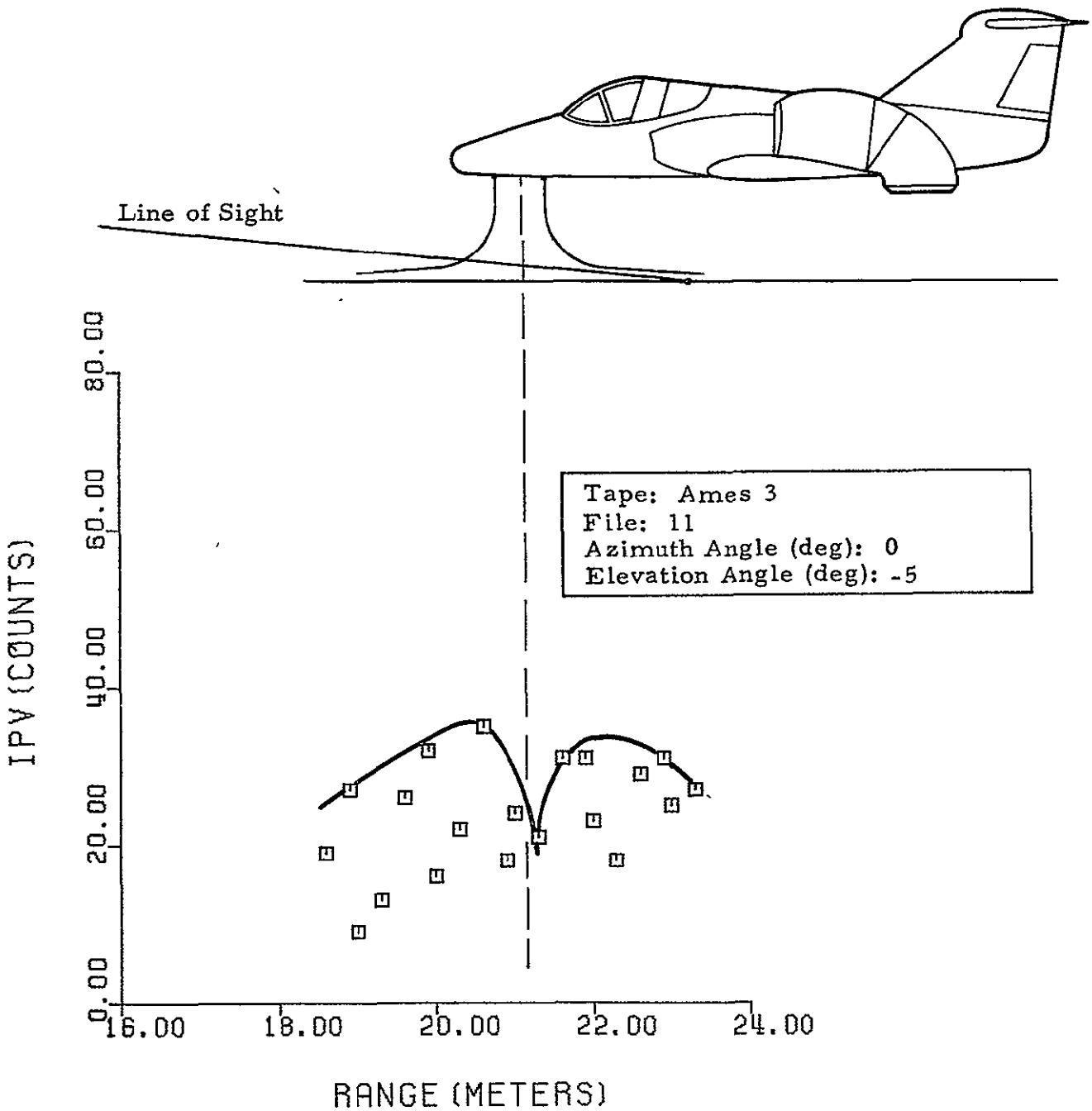

Fig. 12 - Sample Output from ANDKEN Program Showing Distribution of Horizontal Velocity in Wall Jet from Nose Fan

output of the ANDTRN program is shown in Fig. 13. The velocity distribution shows five or six data points along each vertical station below the nose fan. Each data point is computed from approximately three sampling points. The variations in the velocity distributions suggest that an insufficient number of sampling points is available for accurate determination of the velocity field. The lack of sampling points is attributed to the relatively short records (on the order of 60 sec) and to the coarse range scan limits dictated by hardware considerations. For example, approximately 15% of the sampling points fell within the region between the ground and the nose fan. The remaining sampling points were outside the field of interest.

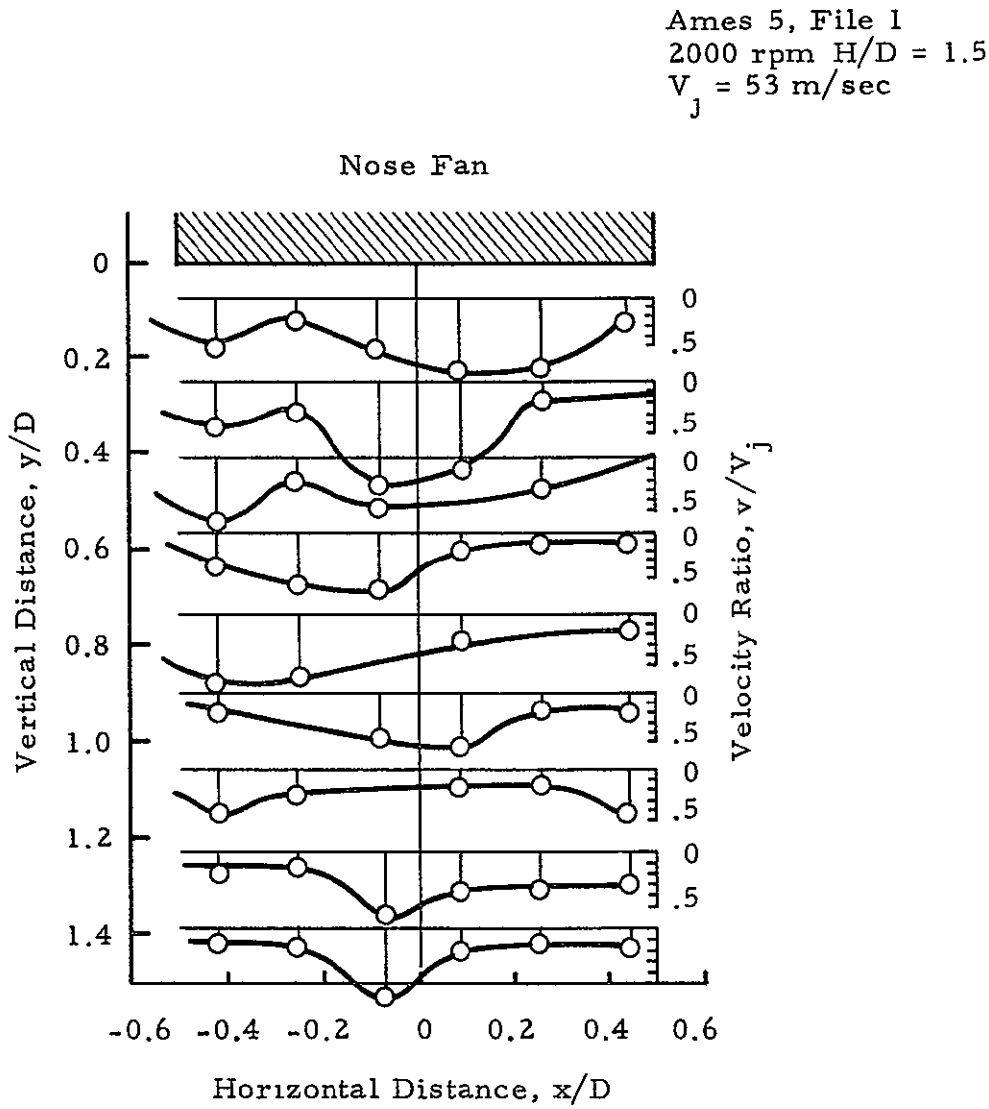

Fig. 13 - Sample Output from ANDTRN Program Showing Distribution of Vertical Velocity Below Nose Fan Along Aircraft Centerline

3. DESCRIPTION OF EXPERIMENTAL TESTS

A two-week test program was carried out with the mobile LDV system deployed at the NASA-Ames static test stand facility. The first week of testing was devoted to setting up, checking out and calibrating the LDV system. During this time the traverse assembly was also set up and calibrated. The signal from the traverse indicating the position of the remote mirror was fed into the PDP 11/34 computer and was logged and processed along with the LDV measurements. The second week of testing was devoted to the survey of the V/STOL flow field including the fan jet exhaust, wall jet decay, fountain vertical velocity, and flow along the aircraft underside.

3.1 TEST PROGRAM

During the LDV flowfield measurement tests, the 70% V/STOL aircraft model was operated over a range of thrust settings (2000 to 4000 rpm) for three different configurations (basic configuration, basic configuration with lift improvement device (LID) and basic configuration with hemispherical hub on nose fan) and two different ground heights (1.5 and 3 m). The test conditions for the flowfield surveys are summarized in Table 1. Additional information on the test program as well as force, moment, pressure and temperature measurements from the aircraft are summarized in Refs. 7 and 8.

3.2 OPERATION OF THE LASER DOPPLER VELOCIMETER

The LDV system was located along the aircraft centerline at a distance of 21 m from the center of the nose fan as sketched in Fig. 14. From this position the LDV surveyed the flow field of the V/STOL aircraft by focusing its sensing volume at different range, azimuth and elevation angle settings. The scan patterns utilized during the test sequence are summarized in Table 2.

Table 1

TEST CONDITIONS FOR FLOWFIELD SURVEYS WITH LDV SYSTEM

Run	δ	Date	Configuration	Acft Ht (m)	Fan rpm			Flowfield Survey	Start Time	End Time	Tape	File
					Nose	Left	Right					
25	2	14 Jul	3-Sided LID On	1.5	2000	2000	2000	Wall Jet of Nose Fan	10:29:00	10 31:40	Ames 2	1
	3				2400	2400	2400		10 32:30	10 37 00		2
	4				2800	2800	2800		10·37 05	10 41·57		
	5				3200	3200	3200		10:42:28	10.45:14		
	6				3500	3500	3500		10:46 37	10 48 57		
26	2	15 Jul	Basic Config., Rails On	1 5	2000	0	0	Wall Jet of Nose Fan	06:40:33	06 41:12	Ames 3	2
									06:41:32	06·41:44		3
									06:42 04	06.42:14		4
									06:42:50	06.42:59		5
	3				2400				06:43·48	06:45:13		6
									06:45 41	06 46:26		7
	4				2800				06·47 36	06·48:17		8
									06 49:02	06 49 22		9
	5				3200				06:51 02	06:51:29		10
					3600				06 53 16	06 53:56		11
	7				4100				06:56 15	06:56:47		12
									06:59:42	07 00 08		13
	8				0	2000	0		07 05 12	07 05 36		14
	9					2400			07·08:01	07:08 39		15
	10					2800			07 11 15	07:12·10		16
	11					3200			07:14 14	07:14 52		17
									07 16:51	07:17 11		21
	12					3600			07 17.20	07:17:48		22
	12				0	3600	0		07·19:57	07:20 41		24
	13					4000			07:20 41	07 20 48		25
	14				0	2000	2000		07.27:11	07:27:52		27
	15					2400	2400		07 31:10	07·31 36		29
	16					2800	2800		07 34 22	07·35·08		30
	17					3200	3200		07 38:06	07.38·39		31
	18					3500	3500		07 41·34	07:42:26		32
27	2				0	0	2000		08 05:33	08:06:17		33
	3						2400		08 09:34	08:10 28		34
	4						2800		08·11:54	08:12 12		35
	5						3200		08:13 47	08 14:45		36
	6						3600		08·17:20	08:18:05		37
	7				2000	2000	2000		08 24 52	08:25 31		38
	8				2400	2400	2400		08 28:27	09·29 07		39
									08 30 21	08·30 57		40
	9				2800	2800	2800		08 32:21	08.32 50		42
	10				3200	3200	3200		08 36 11	08:37·10		43
									08 39:28	08:39 40		44
	11				3500	3500	3500		08 40 18	08 41:14		45
					Idle	Idle	Idle		08 46-24	08:46 50		46
									08:50:03	08:50:22		47
					Off	Off	Off		08.53:54	08 54 09		48
									09:03:15	09 03:15		49
28	3	17 Jul	Basic Config., Rails On	1.5	2400	0	0	Wall Jet of Nose Fan	06 30:13	06:30:33	Ames 4	12
									06:30 40	06 31·07		13
					2400	0	0		06 31 41	06:31 41		14
									06·31.48	06.32:11		15
	4				2800	0	0		06 33:02	06.33:34		16
									06:33.48	06:34 16		17
									06·34:24	06:34:46		18
									06.34 53	06:35:14		19
									06 35:21	06:35 31		20
	5				3200	0	0		06:36:15	06:36 42		21
									06:36·51	06:37:24		22
									06 37:35	06:37 58		23
									06 38·06	06:38:24		24
	6				3600	0	0		06:39:10	06:39:52		25
									06.40:01	06·40:32		26
									06 40 41	06 41:13		27
									06·41·21	06 41:46		28
	7				4100	0	0		06 42 45	06 43 23		29
									06:43 31	06:44·10		30
									06 44·20	06:45 13		31
									06·45 23	06:45·52		32
	8				2000	2000	2000		06·50·43	06·51 17		33
									06.51:45	06:52 14		34
									06 52:21	06:52:46		35
									06 52:54	06:53 27		36
									06.53:35	06·54 03		37
									06:54:10	06:54:20		38
					2400	2400	2400		06:56·28	06 57.10		39

OF POOR QUALITY

Table 1 (Continued)

Run	δ	Date	Configuration	Acft Ht (m)	Fan rpm			Flowfield Survey	Start Time	End Time	Tape	File
					Nose	Left	Right					
28	9	17 Jul	Basic Config., Rails On	1.5	2400	2400	2400	Wall Jet of Nose Fan	06 57 20	06 57 52	Ames 4	40
									06:58:05	06·58:55		41
									06·59·02	06 49 29		42
									06·59:36	06 59.54		43
	10				2800	2800	2800		07:00:56	07:01:52		44
									07·02.01	07.02:41		45
									07·02 47	07·03:17		46
									07.03 30	07:04 03		47
									07:04 13	07·04 26		48
	11				3200	3200	3200		07·05 44	07 05 55		50
									07·06:03	07:06 56		51
									07·07:04	07:07:29		52
									07:07:39	07 08.13		54
	12				3600	3600	3600		07·10:09	07·11:06		56
									07:11.18	07 11.52		57
									07:12·11	07 12.54		58
									07·13:03	07 13.32		59
		18 Jul	Hemi Hub on Nose Fan		2000	0	0	Nose Fan Vert. Vel.	06:10 30	06·11 31	Ames 5	1
					2400				06·11·31	06:11 56		2
					2800				06 12:45	06·13:58		3
					3600				06·15:07	06:16:26		4
					2000	2000	2000		06:18:18	06 19 41		5
									06 20.39	06 20:48		6
									06:20:49	06:21:06		7
	6				2800	2800	2800		06:22.04	06·23·11		9
					3400	3400	3400		06:23·52	06:25 08		10
30	3	19 Jul	Hemi Hub on Nose Fan	3.0	2400	0	0	Azi. Scan Under Acft	09 51:43	09·52:50	Ames 6	2
	4				2800				09 54 16	09:55:07		3
									09.55:22	09:55:54		4
									09 56:08	09·56:36		5
	5				3200				09 58:42	10:00:01		6
	6				3600				10·01 35	10:02:11		7
									10 02:21	10 02.43		8
									10 02:55	10:03 30		9
	7				4100				10.04 29	10:05 06		10
									10 05:21	10:05 43		11
									10:05:59	10·06 43		12
	8				2000	2000	2000		10 12:16	10 13:01		13
									10 13:15	10 13 40		14
									10:14 08	10 14:30		15
	9				2400	2400	2400		10·15:52	10:16:34		16
									10.16:47	10:17:14		17
									10.17·37	10:18 07		18
	10				2800	2800	2800		10:19:21	10:19 53		19
									10 20·10	10:20 44		20
									10 20:57	10 21·35		21
					3200	3200	3200		10 22·44	10:23:12		22
									10:23:23	10·23 50		23
30A				3.0	0	2000	2000	2-Jet Fountain	12·59:57	13 02 06	Ames 7	1
									13:02:07	13:02·12		2
						2400	2400		13 03:38	13 06.02		3
						2800	2800		13 07:10	13.08:20		4
									13 08 30	13.10·27		5
						3200	3200		13·12:01	13·12 33		6
									13·12:34	13·13 25		7
									13·13:26	13:15:16		8
						3600	3600		13:16 06	13.18:36		9
									13:18:36	13·19:23		10
						3600	3400		13:20:26	13 24 07		11
						3600	3200		13 25:21	13:28 22		12
									13.28:23	13·28 41		13
						3600	2800		13.30 05	13 33:57		14
						3400	3600		13 35:27	13:36:32		15
						3600	2800	2-Jet Fountain	15 00:35	15 03 42	Ames 8	1
						3600	3200		15 04:51	15:06:15		2
									15 06:15	15 08 00		3
						3600	3400		15 08:46	15 11:54		4
						3400	3400		15 12:57	15:16:19		5
30B		19 Jul			2800	2800	2800		15:18 43	15 21:59		6
									15·22·05	15:22:05		7
									15:22:25	15·22 46		8
									15:22:54	15:23 07		9
									15·23:38	15·24 01		10

Table 1 (Concluded)

Run	δ	Date	Configuration	Acft Ht (m)	Fan rpm			Flowfield Survey	Start Time	End Time	Tape	File
					Nose	Left	Right					
30B	10	19 Jul	Hemi Hub on Nose Fan	3.0	3000	3600	3600	2-Jet Fountain	15:26:02	15 28:49	Ames 8	11
									15:29:07	15·30:06		12
									15:30 12	15 30·45		13
									15:30.52	15 31:13		14
									15:31:19	15 31·36		15
									15 31.42	15 31 50		16
31	5	20 Jul	Basic Config	3.0	3200	0	0	Wall Jet Stag. Flow	06:45:13	06 46 43	Ames 9	1
	6				3600				06·47:24	06·49 31		2
	7				4100				06·50:22	06:52 01		3
	8				2000	2000	2000		06:59·08	08:59 45		4
	9				2400	2400	2400		07:00:33	07:02:04		5
	10				2800	2800	2800		07.04:07	07:05:51		7
	11				3200	3200	3200		07:07·55	07:10 19		8
	12								07 11:40	07:13:01		9
									07 13:51	07:15·27		10
									07·15:52	07:17·28		11
32	2	20 Jul	Basic Config.		0	2000	0	Rear LC Wall Jet	07:43 06	07:44:21		12
	3					2400			07:45:36	07:47:36		13
	5					3200			07·48 10	07:49:35		14
									07 50 50	07:52·42		15
	6				0	3600	0		07 53:28	07:54 50		16
	7					3950	0		07:56 11	07·57 47		17
	8					2000	2000	Fuselage Flow	08·04:50	08·05 24		18
	9					2400	2400		08.06:11	09:07 45		19
	10					2800	2800		08:10:08	08:11:29		20
	11					3200	3200		08 12.22	08:13 44		21
									08.15:02	08.15:22		22
	12					3600	3600		08·16:06	08 16:56		23
									08 18:11	08 18·35		24
								Wall Jet	08 18 56	08·19:29		25
									08 19:39	08·20·01		26
									08 20 36	08·21:31		27
	13					0	2000	Wall Jet Right L/C	08 26·13	08:26:45		28
	14						2400		08 28 20	08 29:21		29
							2800		08:31·29	08 32:37		30
							3200		08:34:07	08·35:24		31
							3600		08.37 09	08·38 32		32
33A	1	20 Jul	3-Sided Lid On	3.0		2800	2800	2-Jet Fountain	12.58 25	12:59 12	Ames 10	1
									12.59 12	13:00 22		2
									13.00.22	13.01·23		3
	2				0	3600	3600		13:02:26	13:05 58		4
	3					3600	3200		13.07·17	13:09:05		5
									13:09:05	13:10 22		6
						3600	2800		13 11:11	13:11·37		7
									13 11:37	13:12:55		8
	4				3200	3200	3200		13:28 26	13:28·48		10
									13·28:49	13.31 37		11
					3600	3600	3600		13·33·08	13:36 24		12
	5				3600	3200	3200		13:37:29	13 40·36		13
	6				2200	2800	2800		15:05:38	15·08 20		16
									15 08:21	15:08 57		17
					3600	3600	3600		15 22:28	15:23:48		22

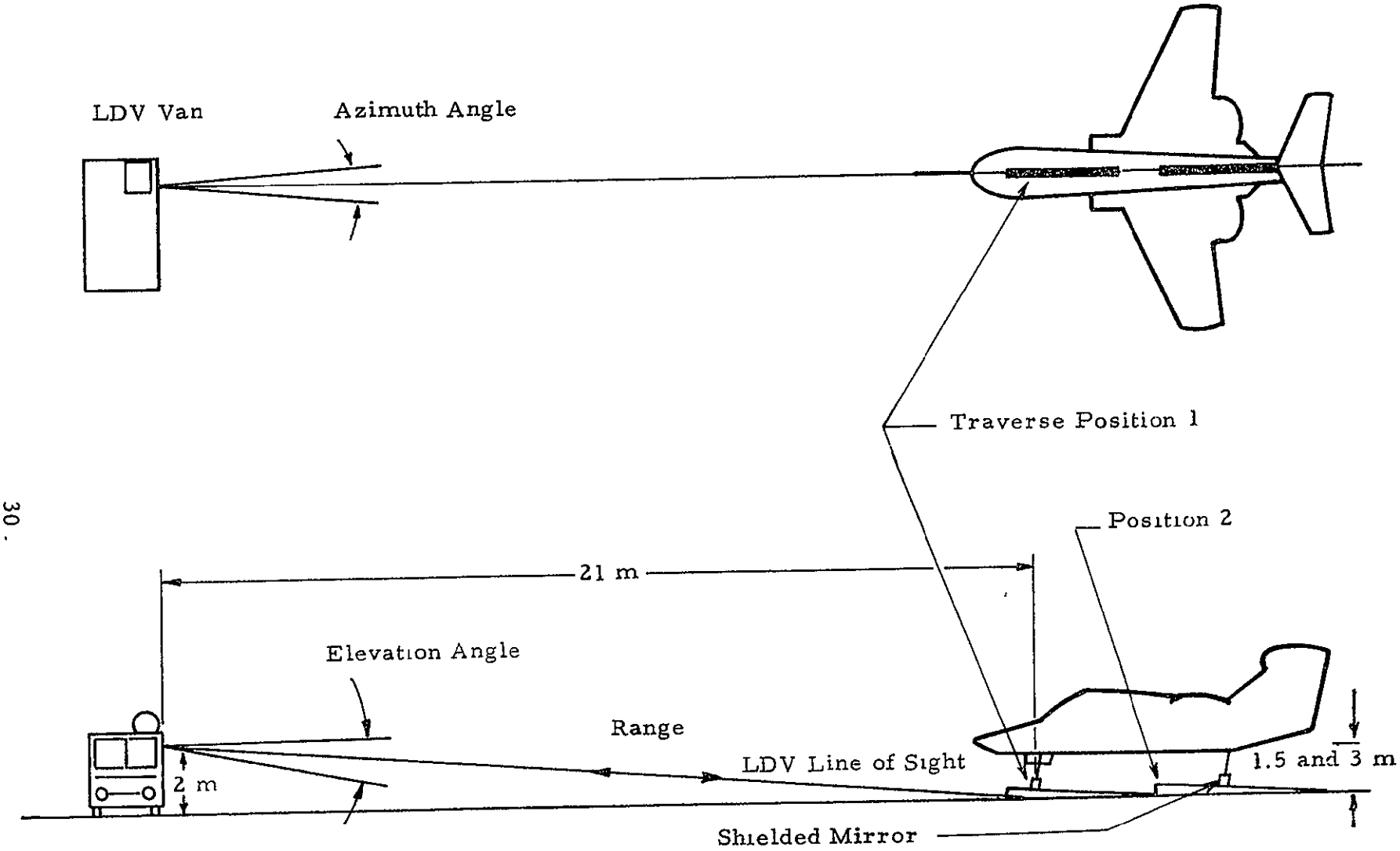

Fig. 14 - Deployment of LDV System at NASA-Ames

Table 2

SCAN PATTERNS UTILIZED DURING V/STOL TEST

No.	Range (Variable) (m)	Azimuth Angle (deg)	Elevation Angle (deg)	Comments
1	18-28	Fixed, 0	Fixed -5.5	Beam focused at region of maximum horizontal velocity.
2	18-28	Fixed, 0	Var., -4, -6	Investigate vertical dimension of ground jet.
3	18-28	Fixed, 0	Discrete, -4, -5, -6	Investigate lateral dimension of ground jet.
4	25-35	Var., 1-359	Discrete, 0	Investigate lateral dimension of ground jet.
5	18-28	Fixed, 0	-4.6	Survey of vertical velocity of nose fan — traverse in Pos. 1.
6	25-35	Fixed, 0	-3.25	Survey of vertical velocity of fountain — traverse in Pos. 2.

It is noted that these scan patterns use only the side view window of the LDV and represent only a small fraction of the full three-dimensional LDV scan capabilities (see Fig. A-6, Appendix A). Modifications to the test site or to the existing LDV scanner would enable use of the overhead scanner and would produce full three-dimensional scans. The scan patterns summarized in Table 2 provided the capability to investigate the horizontal velocity of the wall jet, vertical velocity distribution in the nose fan and two-jet fountain, and the horizontal velocity along the aircraft underside.

Since the LDV provides an absolute measurement of velocity, i.e., the Doppler shift is a direct measure of the magnitude of the line-of-sight velocity, no calibration of velocity was necessary during field operations. To check the range calibration and optical alignment of the system before and after each test sequence, the LDV was periodically focused on a spinning sandpaper disk target placed at a fixed range. The LDV was operated in the range scan mode

and the spatial resolution of the system was deduced from the variation in the observed signal-to-noise ratio of the wheel target versus range. During the tests, the hard target was also placed behind the hot jet engine exhaust as sketched in Fig. 15. Less than a 1/2 dB difference was seen in the peak signal-to-noise ratio from the wheel with and without the jet exhaust and no significant change was seen in the range resolution. The range resolution is defined as the range interval over which the return signal from a hard target decreases to one-half its value (see Fig. A-6, Appendix A). The results suggest that defocusing due to turbulence and temperature gradients was negligible at idle rpm. The spinning disk was also used to check the alignment of the laser beam during the runs utilizing the traverse and remote mirror assembly. Measurements before and after each run showed that the LDV system maintained alignment through the remote mirror assembly.

Typical Return Signal from LDV

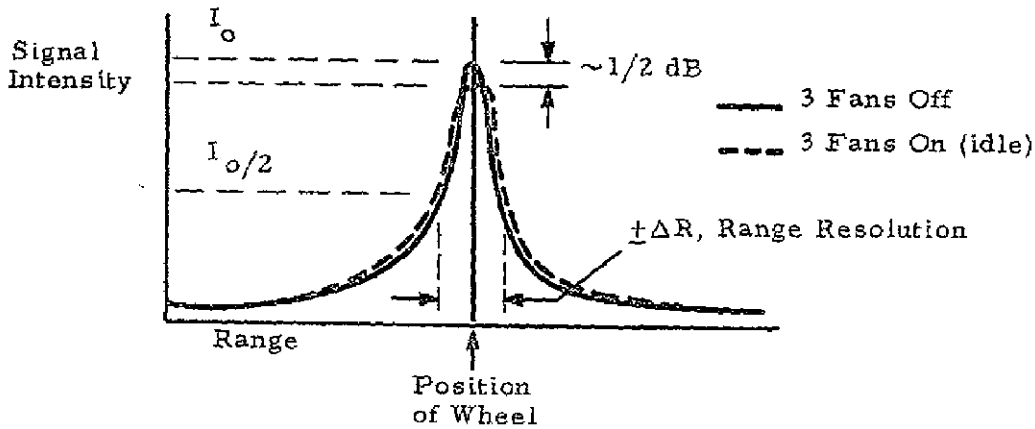

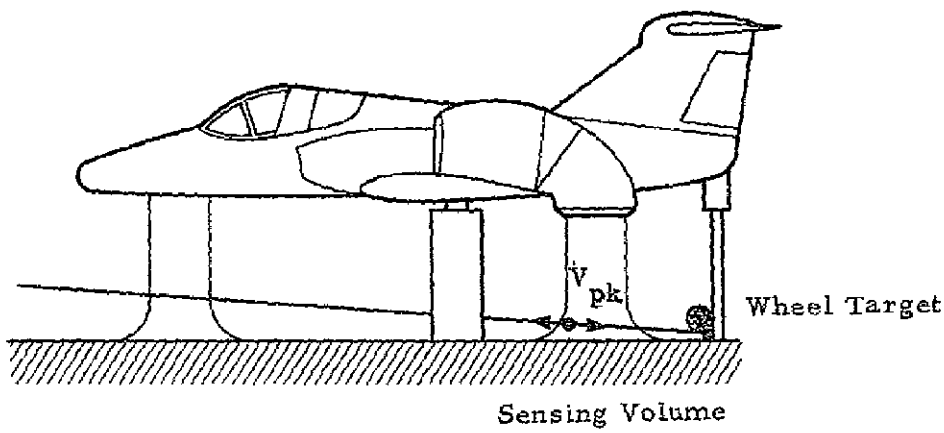

Fig. 15 - Sketch of Test to Investigate Influence of Temperature and Turbulence Gradients on Return Signal

4. RESULTS OF LASER DOPPLER VELOCIMETER MEASUREMENTS

Flow field measurements obtained with the LDV system are discussed below including the characteristic velocity distribution in the wall jet, fan jet, fountain and fuselage flow. A listing of all of the LDV velocity surveys is given in Appendix B.

4.1 CHARACTERISTIC VELOCITY SIGNATURE

The typical velocity signal from the LDV during a survey of the wall jet of the V/STOL aircraft is shown in Fig. 16. The signature, taken over a 1/70 sec sampling time, shows the backscatter intensity versus Doppler shift frequency (velocity) from particles within the sensing volume of the LDV. The velocity corresponding to the highest amplitude, V_{pk}, is representative of the mean velocity of particles in the sensing volume. The highest velocity above the amplitude threshold, V_{max}, is representative of the maximum velocity observed. The amplitude and frequency thresholds are adjusted to filter out the background noise of the system. Note that for the typical sample case shown in Fig. 16 the difference between the mean and maximum velocity is large, $\Delta V = (V_{max} - V_{pk})/V_{pk} = 41\%$. This is indicative of large gradients in the flow and high turbulence levels. The area under the intensity frequency curve, ISUM, is a measure of the total scattering cross-sectional area of particles within the sensing volume and is a function of the relative particulate concentration in the flow, ρ. The total bandwidth of the signal is given by the number of filled velocity bins, N, and is a function of the particulate concentration and turbulence in the flow. The signature from the LDV survey of the V/STOL flow, shown in Fig. 16, is similar to the typical LDV output illustrated earlier in Fig. 7.

The magnitude of the instantaneous line-of-sight velocity, $|V_{pk}|$, as a function of range for scans through the wall jet of the nose fan is illustrated

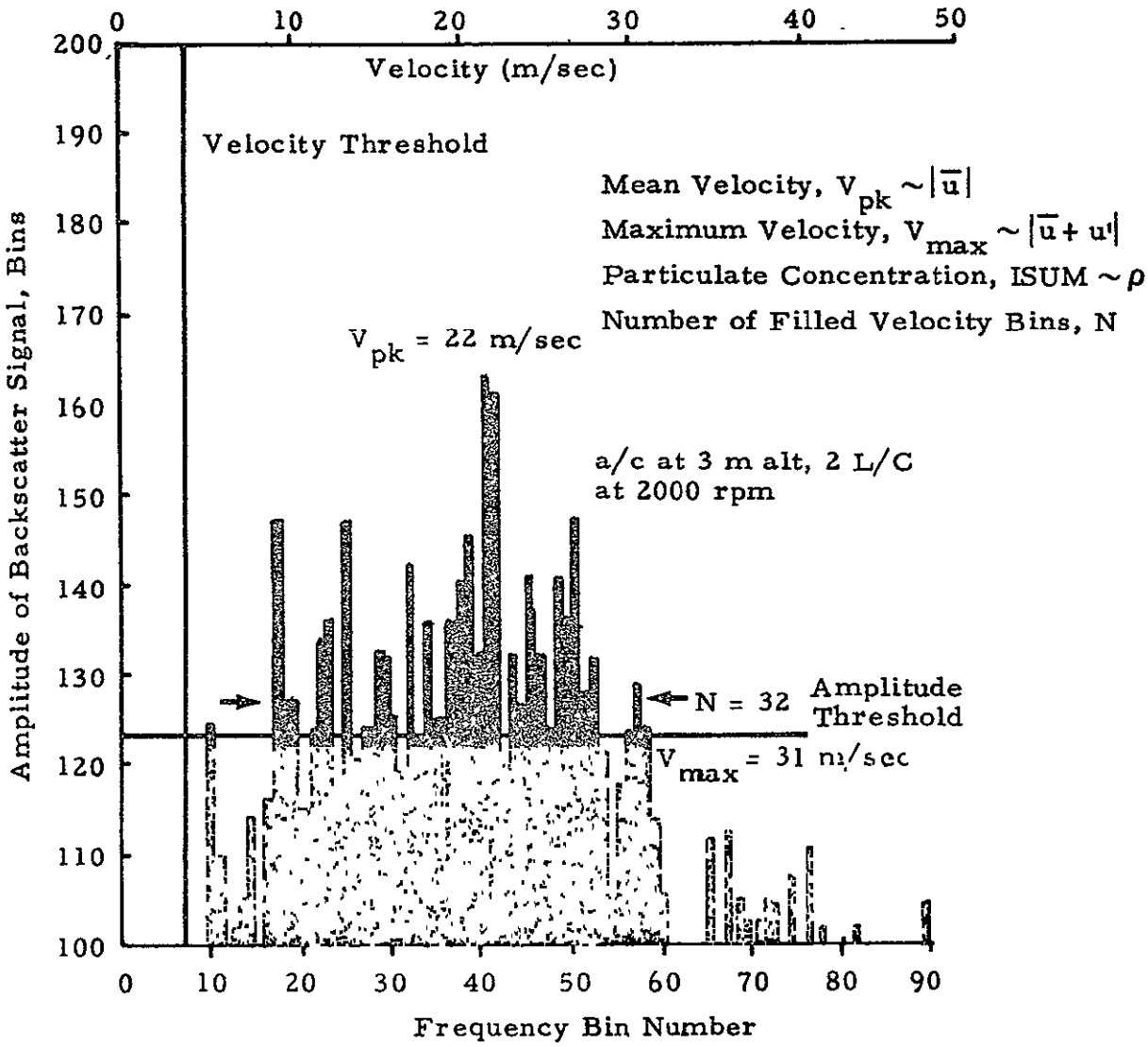

Fig. 16 - Signature from LDV During Survey of Wall Jet of V/STOL Aircraft

ORIGINAL PAGE IS
OF POOR QUALITY

in Fig. 17. The geometry for the range scan measurements is sketched in the top of the figure. The LDV was aligned with the aircraft centerline and the elevation angle of the line of sight was adjusted until the maximum radial velocity was observed in the wall jet. This occurred at -4.4 deg elevation angle from the side window of the LDV van so that the beam hit the ground at 5 m from the jet centerline as shown in Fig. 17. The LDV was scanned in range through the wall jet approximately once every second producing a series of line-of-sight velocity profiles. The start time and direction of each range scan is labeled in Fig. 17. The typical range resolution of the LDV is given by the length of the sensing volume and is indicated on the bottom of the figure. The sequential line-of-sight velocity profiles show that the horizontal velocity ratio $\dot{u}/V_j$ ranges from 0.12 to 0.86 in the region 0.5 to 1.5 jet diameters from the jet centerline and within 0.2 to 0.5 diameters above the ground. The reference jet exit velocity, V_j, is taken from measurements obtained from an internal fan mounted pressure rake. Comparing sequential velocity profiles, there is evidence of a large degree of unsteadiness in the flow.

The large fluctuations in the line-of-sight velocity were observed throughout the experiment and are attributed primarily to the high turbulence levels in the flow. However, it is recognized that the relatively long focal volume of the LDV in comparison to the spatial gradients in the flow field and an uneven distribution of aerosols can also contribute to fluctuations in the observed line-of-sight velocity distribution.

The magnitude of the instantaneous signal from the LDV is indicated in Fig. 18. The signal levels are indicative of the ability of the LDV to track the movement of the particulates in the flow. The amplitude of the backscattered signal, ISUM, is high (typical signal-to-noise ratio is 20 dB) and the signal strength varies considerably with time and range as shown by the plots given in Fig. 18. The occurrence of dropouts (signal intensities below the threshold of the system) is low, indicating that a sufficient number of particles exist at essentially all times within the focal volume for monitoring the flow field. The localized high backscatter regions at various distances from the jet centerline suggest nonuniform seeding of the flow. Puffs of smoke were observed

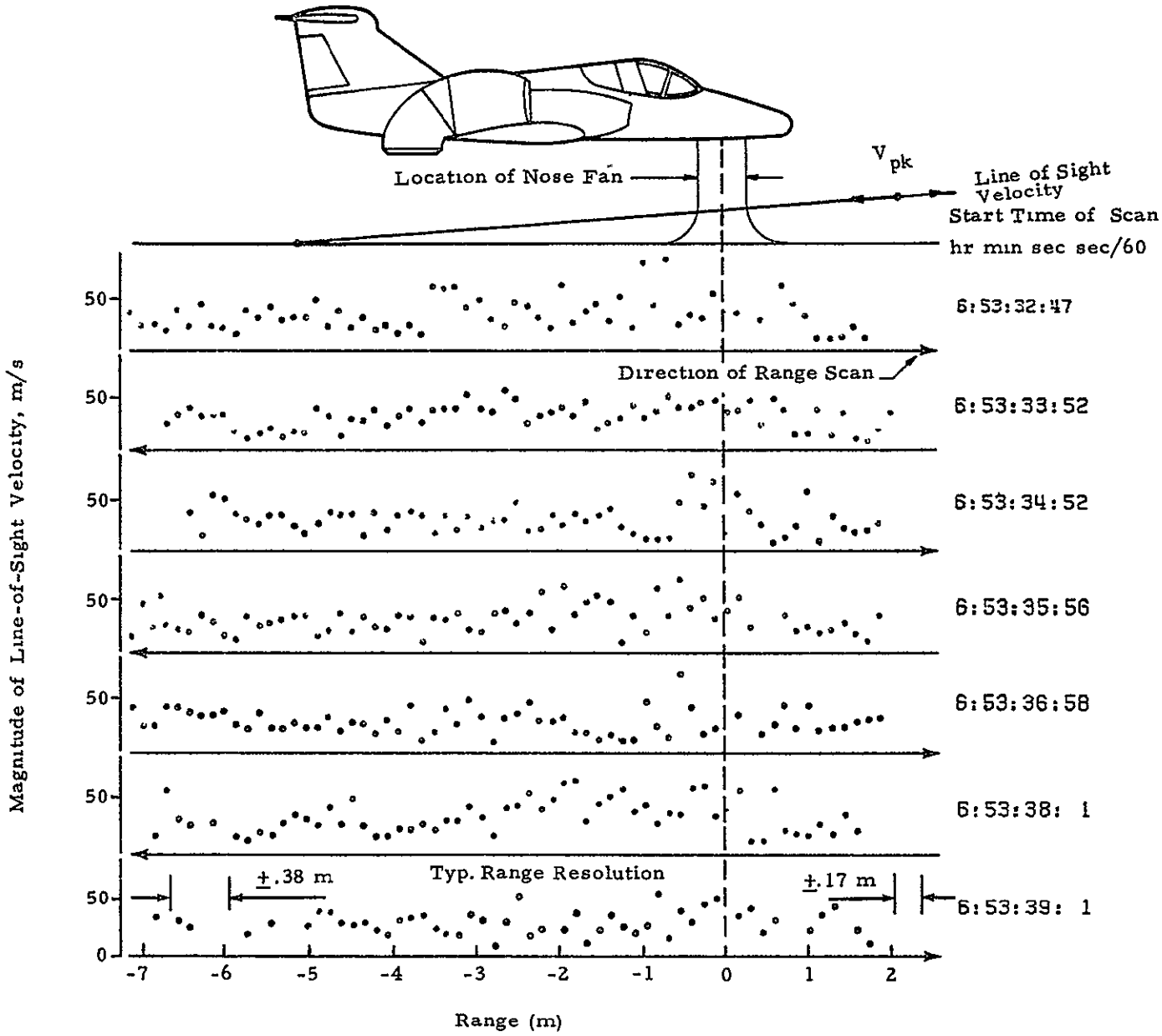

Fig. 17 - Magnitude of the Line-of-Sight Velocity as a Function of Range for Scans Through the Wall Jet of the Nose Fan at 3600 rpm for Aircraft Height of 1.5 m

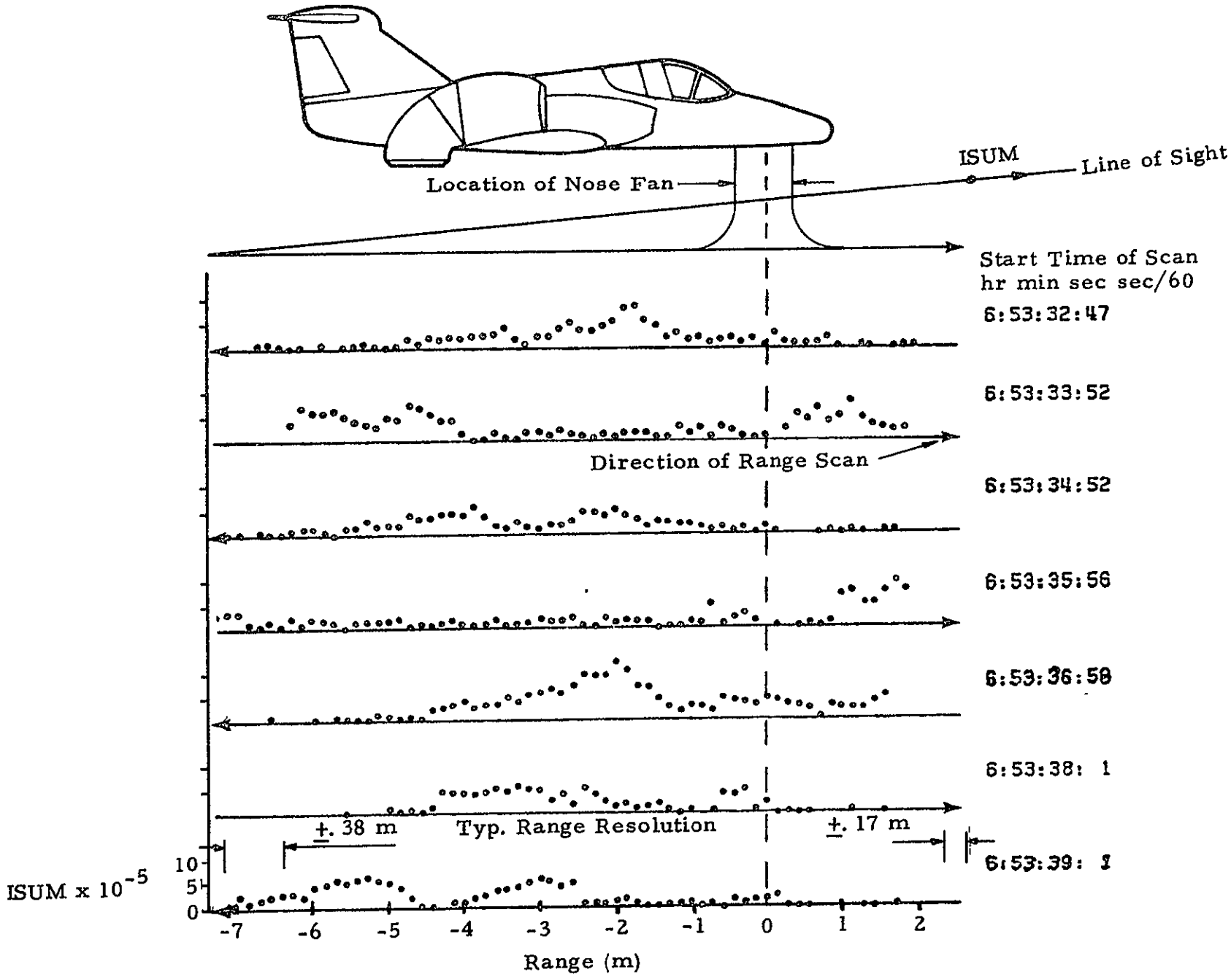

Fig. 18 - Magnitude of the Backscatter Intensity, ISUM, as a Function of Range for Scans Through the Wall Jet of the Nose Fan, Aircraft Height 1.5 m, Nose Fan at 3600 rpm

occasionally during the tests. It is conjectured that this is the reason why ISUM is not consistently maximum at the centerline of the jet.

Since the LDV system depends upon optical focusing for range scanning, the nonuniform seeding can degrade the spatial resolution of the system. Particles outside the nominal focal volume may have a sufficient backscatter intensity to register on the system.

Another characteristic of the LDV signature is the frequency range of the signal or the number of frequency bins containing acceptable data. The number of data acceptables, N, gives an indication of the gradients in the flow and the degree of turbulence and the concentration of particulates in the flow. For a given velocity field, the higher the relative particulate concentration the higher the number of data acceptables. Thus, the number of data acceptables contains information on both the velocity gradients and particulate concentration in the flow. A typical distribution of the number of data acceptables as a function of range is given in Fig. 19. The number of data acceptables varies in a nonuniform manner with range very much like the ISUM plot shown earlier in Fig. 18.

From consecutive range scan measurements discussed above, the velocity field in the near wake of the V/STOL aircraft was determined. Due to the large fluctuations in the instantaneous velocity, different averaging techniques were investigated to identify the mean velocity trends. A comparison of the maximum line-of-sight velocities computed for the wall jet near the ground from the nose fan is illustrated in Fig. 20. The three processing techniques included the computation of the maximum value of V_{pk}, average value of V_{pk} and the maximum value of IPV. For comparison, the maximum velocity measured in a laboratory with a hot-wire in a wall jet is also shown. The results indicate that the maximum value of V_{pk} is in agreement with the magnitude of velocity measured with a hot-wire. The maximum value of V_{pk} and the maximum value of IPV is on the order of 100% and 65% of the magnitude of the hot wire velocity, respectively.

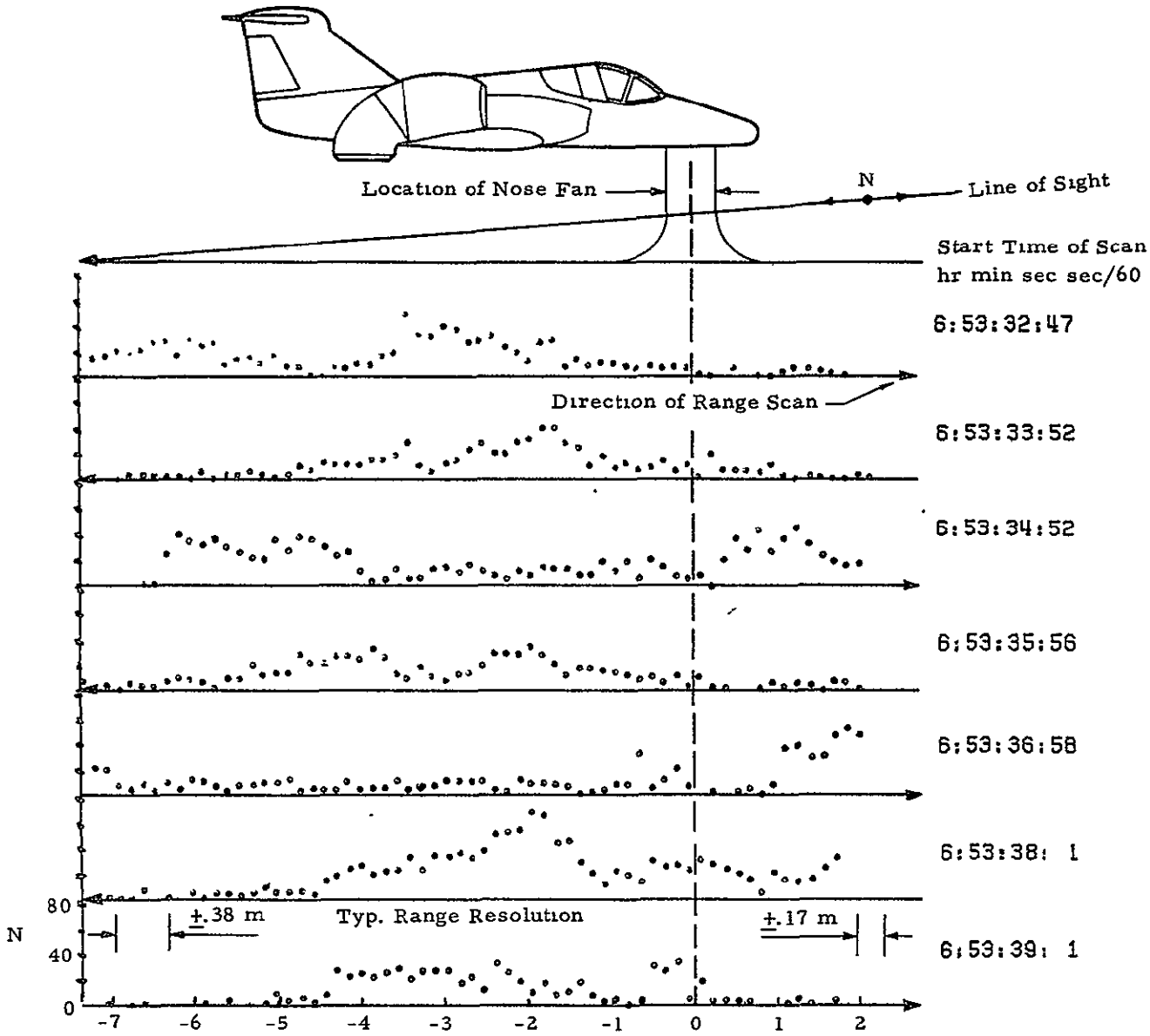

Fig. 19 - Number of Data Acceptables, N, as a Function of Range for Range Scans Through the Wall Jet of the Nose Fan for Aircraft Height 1.5 m, Nose Fan at 3600 rpm

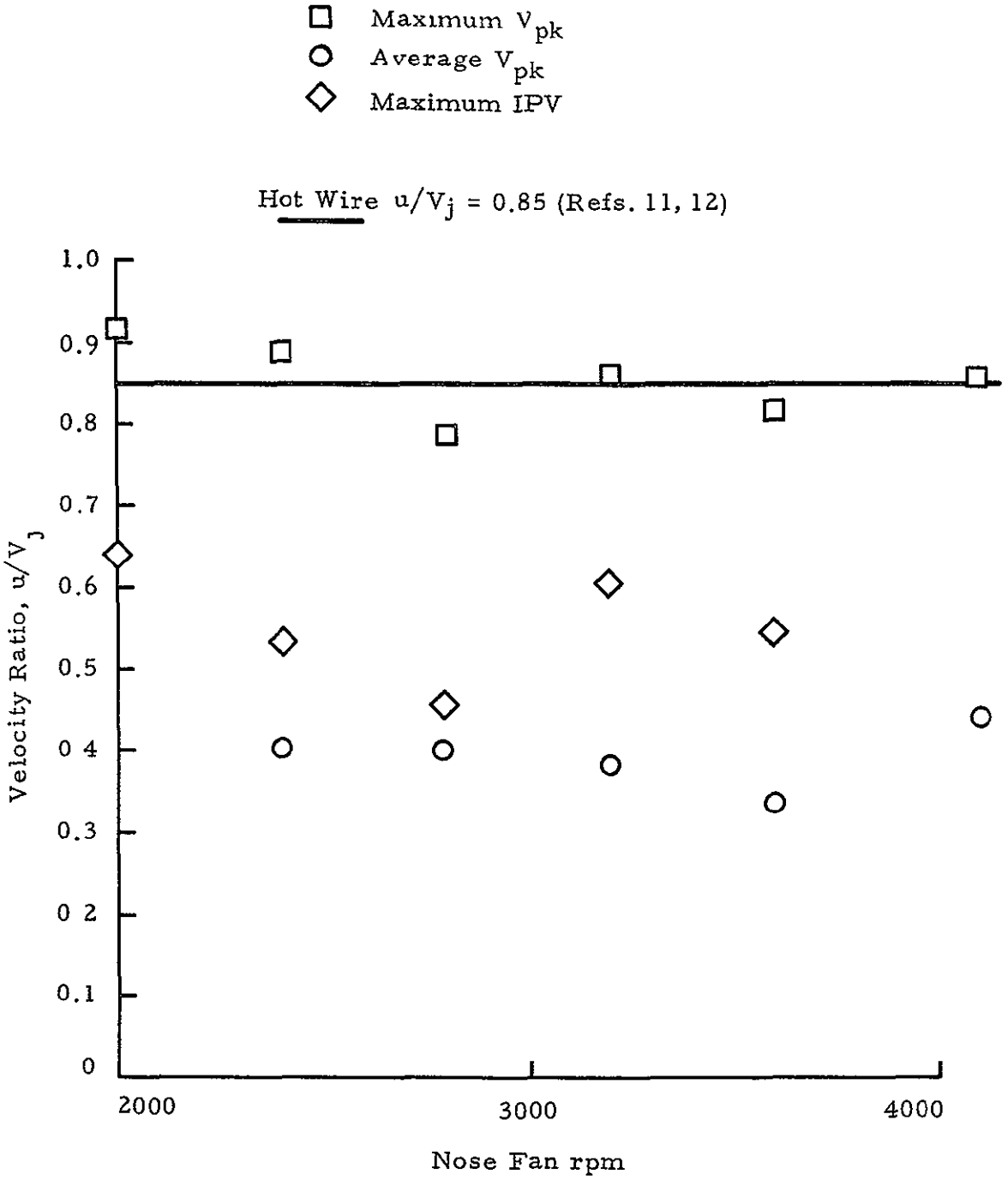

Fig 20 - Comparison of Maximum Line-of-Sight Velocities Computed for Wall Jet Near Ground from Nose Fan

4.2 WALL JET DECAY

The decay of the wall jet near the ground is shown in Fig. 21 for the nose fan. The horizontal velocity distribution was obtained from a series of 60 or more successive 1 sec range scans illustrated earlier. The range excursions were segmented into 100 discrete bins and the maximum value of the line-of-sight velocity was saved in each bin. A curve was faired through the maximum of the values in the bins to eliminate any biases due to a lack of sampling points or particles in the focal volume. The distribution of velocity 0.2 to 0.5 diameters above the ground indicated a peak velocity ratio of 0.85 at approximately one jet diameter from the nozzle exit. For comparison, laboratory measurements obtained on an impinged round jet with a jet Reynolds number Re = 1.6 x 10^5 are included in the figure

The maximum velocity observed near the ground as a function of fan rpm is shown in Fig. 22. The maximum velocity ratio ranges from 0.73 to 0.93 and does not vary consistently with fan rpm, ground height or fan hub geometry for the cases tested. Measurements with a hot wire of a round jet impinging on a flat plate indicate a maximum velocity ratio of 0.85 at a location 1.5 jet diameters from the jet centerline as shown by the solid line in the figure.

4.3 FAN JET

The distribution of vertical velocity along the aircraft centerline at the location of the nose fan is shown in Fig. 23. The velocity distribution was obtained by fairing points obtained from a series of 13 range scans through the traverse mounted remote mirror assembly. The large fluctuations in the measurements, shown by the vertical bars, suggest high turbulence levels in the flow.

The mean vertical velocity at the nozzle exit of the nose fan measured by the LDV and by pitot probes mounted in the fan is presented in Fig. 24. The LDV velocity distribution was obtained by plotting the maximum velocity computed from IPV and V_{pk} versus range curves at each rpm. The velocity

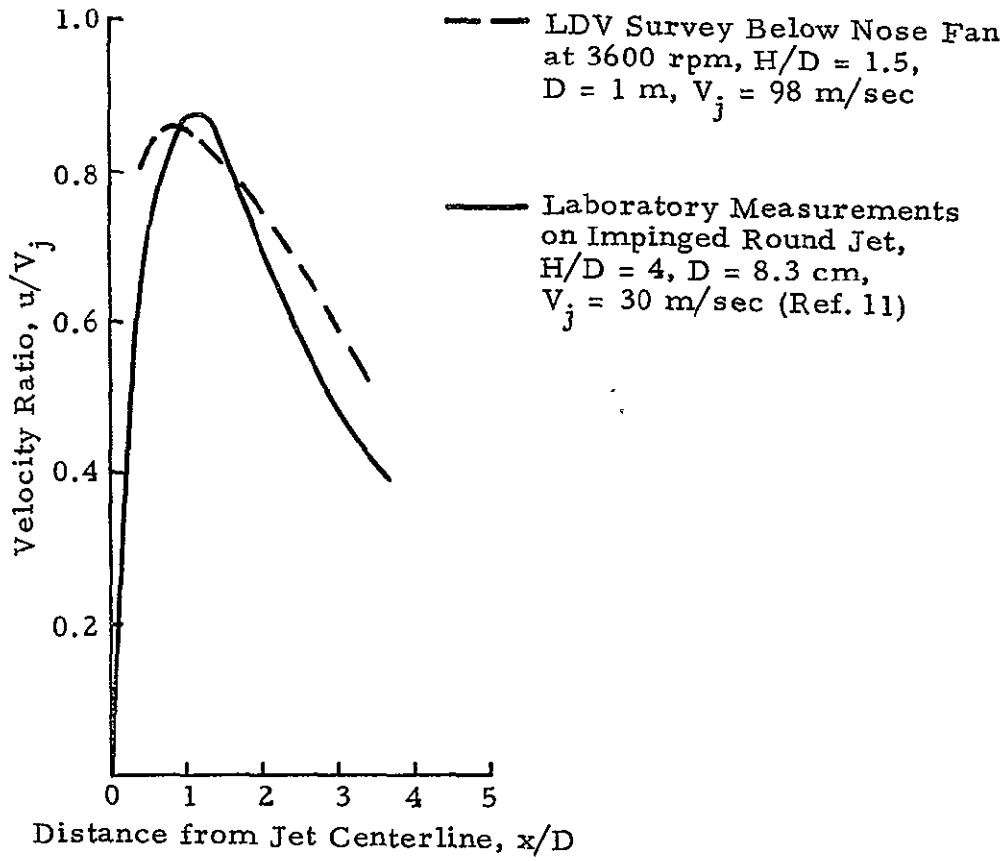

Fig. 21 - Distribution of Peak Velocities Near Ground Below Nose Fan

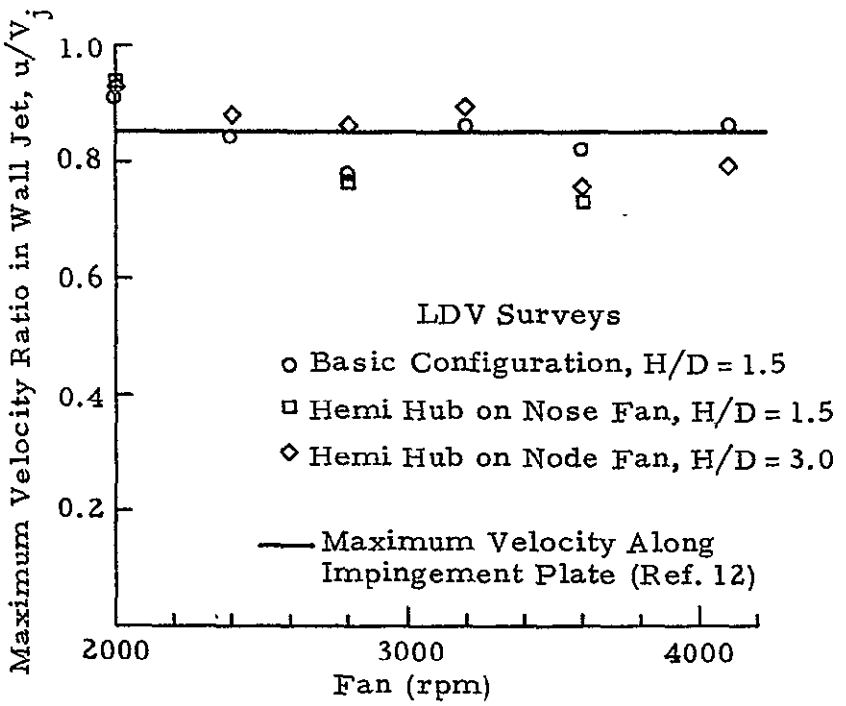

Fig. 22 - Maximum Velocity in Wall Jet as a Function of Fan rpm

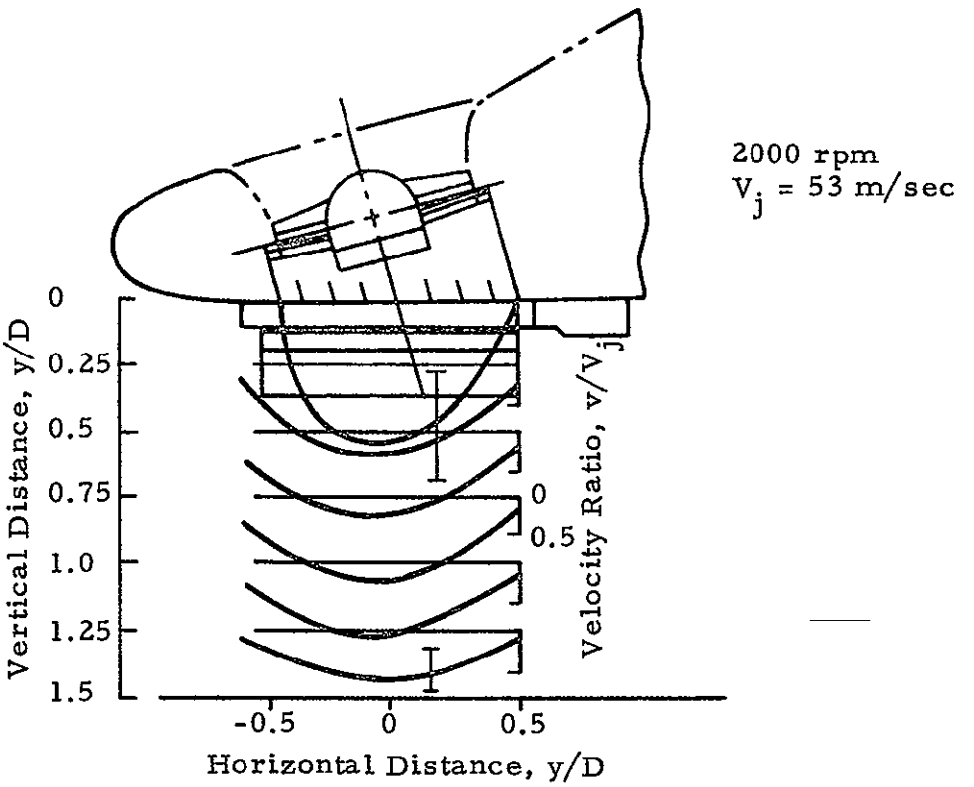

Fig. 23 - Distribution of Vertical Velocity Along Aircraft Centerline at Location of Nose Fan

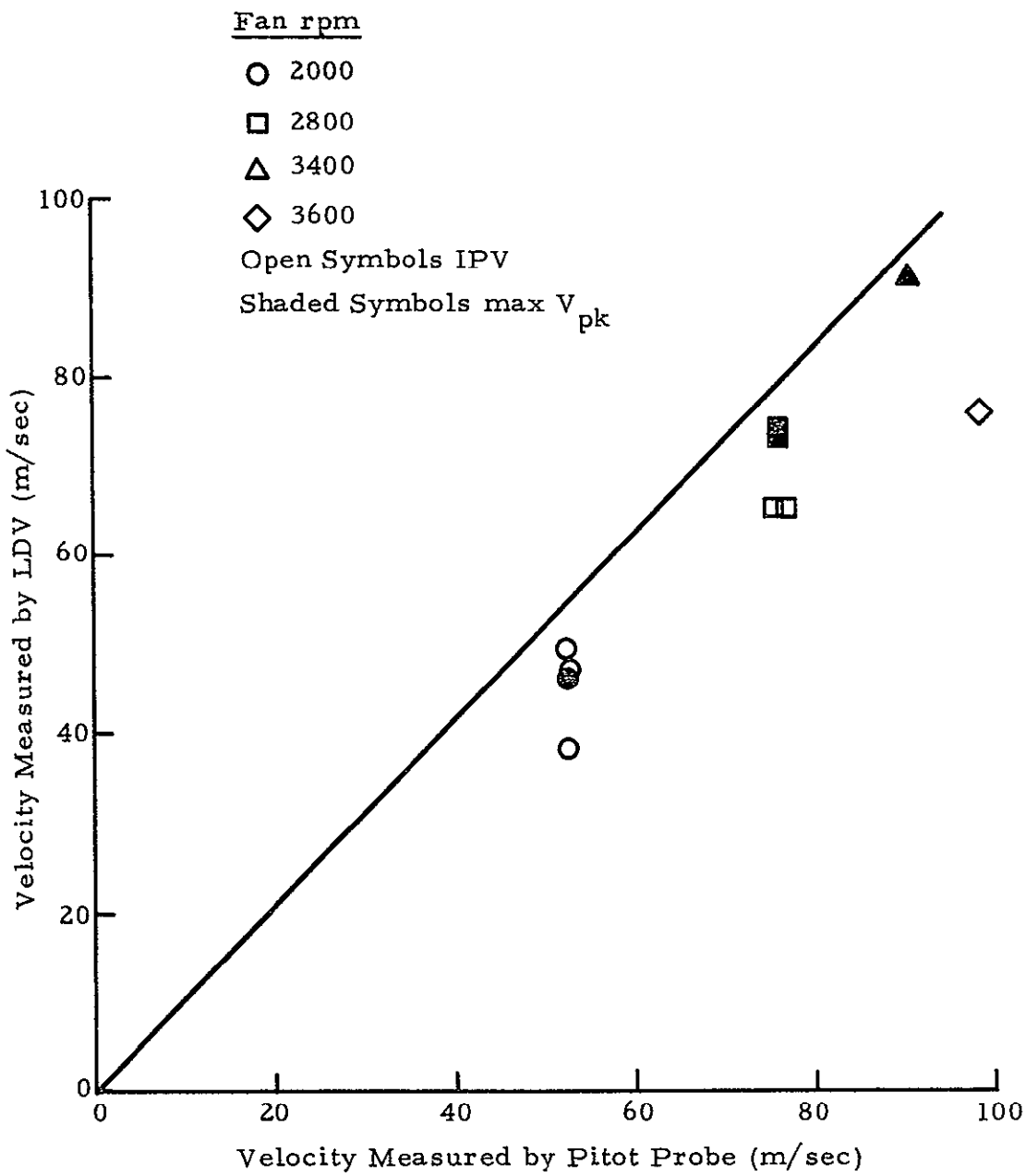

Fig. 24 - Mean Vertical Velocity at Nozzle Exit of Nose Fan Measured by LDV and Pitot Probe

measured by the LDV is generally lower than the velocity measured by the pitot probe. This is attributed to the different location where each measurement was made.

4.4 FOUNTAIN

The distribution of vertical velocity along the aircraft centerline near the ground for the two-jet fountain is shown in Fig. 25. The LDV measurements were obtained by segmenting the traverse location into 40 discrete range bins and by generating a composite frequency (or velocity) spectrum for each range bin. The composite spectrum summed the signal intensity versus Doppler frequency shift contributed from each sample point in that range bin. The frequency shift corresponding to the maximum integrated intensity, IPV, was taken to be the representative velocity for that range bin. The processing technique was developed to minimize variations in the line-of-sight velocity due to an uneven distribution of aerosols in the flow and to compensate for the long focal volume of the system. The results in the figure indicate that the maximum vertical velocity ratio in the two-jet fountain is between 0.4 and 0.5. This high velocity region extends approximately three jet diameters along the aircraft centerline. The velocity ratio and spatial extent of the high velocity region do not change significantly with fan rpm for the configuration tested.

The distribution of vertical velocity as a function of height above ground in the two-jet fountain is shown in Fig. 26. The plot was generated from averaging the measurements of the vertical velocity, IPV, at 10 lateral positions and 10 vertical positions in the fountain. The results show that the maximum vertical velocity ratio in the fountain occurs at 0.3 to 0.4 jet diameters above the ground. The scatter in the measurements is attributed to the turbulence level in the flow and to the averaging of the measurements from different locations in the fountain.

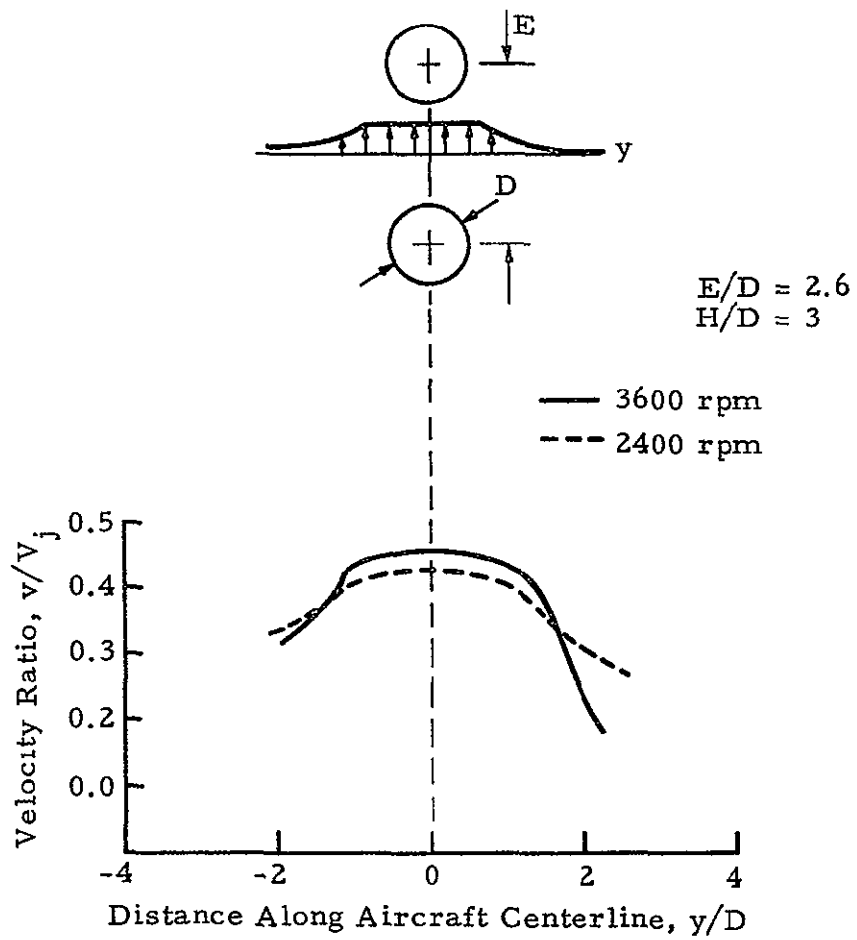

Fig. 25 - Distribution of Vertical Velocity Along Aircraft Centerline Near Ground for Two-Jet Fountain

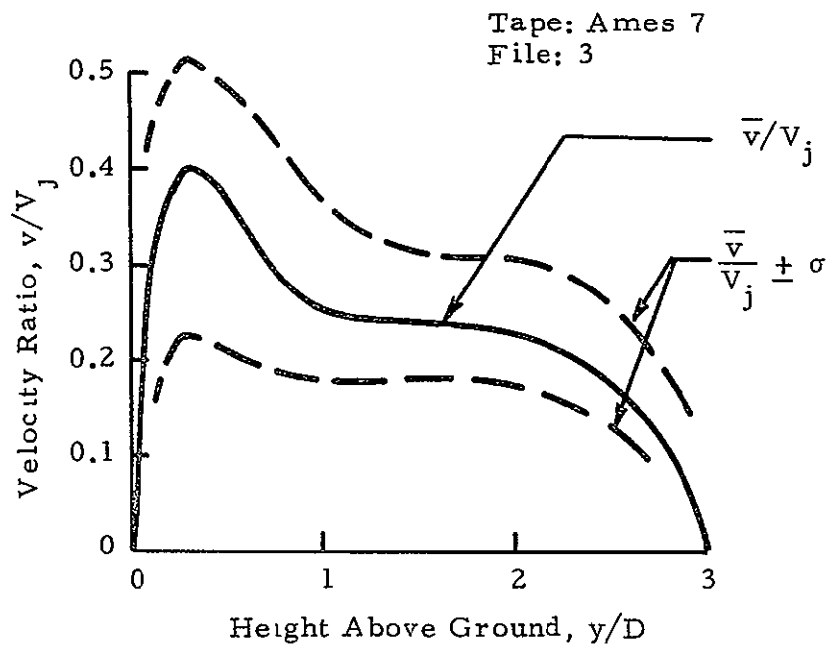

Fig. 26 - Distribution of Vertical Velocity as a Function of Height Above Ground in Two-Jet Fountain

The distribution of the maximum vertical velocity along the aircraft centerline for the two- and three-jet fountain is shown in Fig. 27. The results indicate that a mismatch in engine rpm reduces the maximum velocity ratio in the fountain from 0.46 to 0.39 for the 3600/3600 rpm and the 3600/3200 rpm case, respectively. The maximum vertical velocity is higher and the fountain is tighter for three-jet operation. The results in Fig. 27 show an increase in the maximum vertical velocity ratio from 0.46 to 0.49, and a 22% decrease in the lateral extent of the fountain for the 3600/3600/3600 versus 3600/3600 rpm case.

4.5 FLOW ALONG FUSELAGE

Fuselage Flow

The distribution of the magnitude of the horizontal velocity along the aircraft centerline on the bottom of the fuselage is illustrated in Fig. 28. The LDV measurements were processed using the discrete range composite spectrum technique discussed earlier. The measurements of IPV show two localized high velocity regions with a maximum velocity ratio between 0.1 and 0.2. The high velocity peaks are situated approximately one jet diameter forward and aft of the lift cruise fan engines.

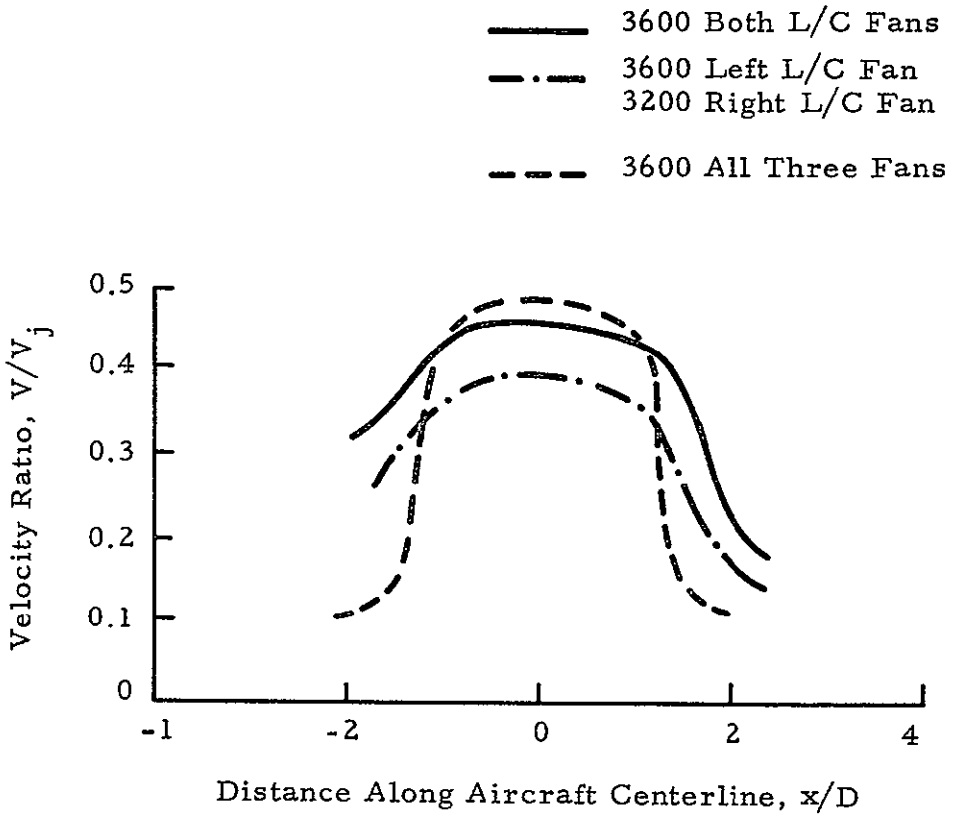

Fig 27 - Distribution of Vertical Velocity Along Aircraft Centerline Near Ground for Two- and Three-Jet Fountain

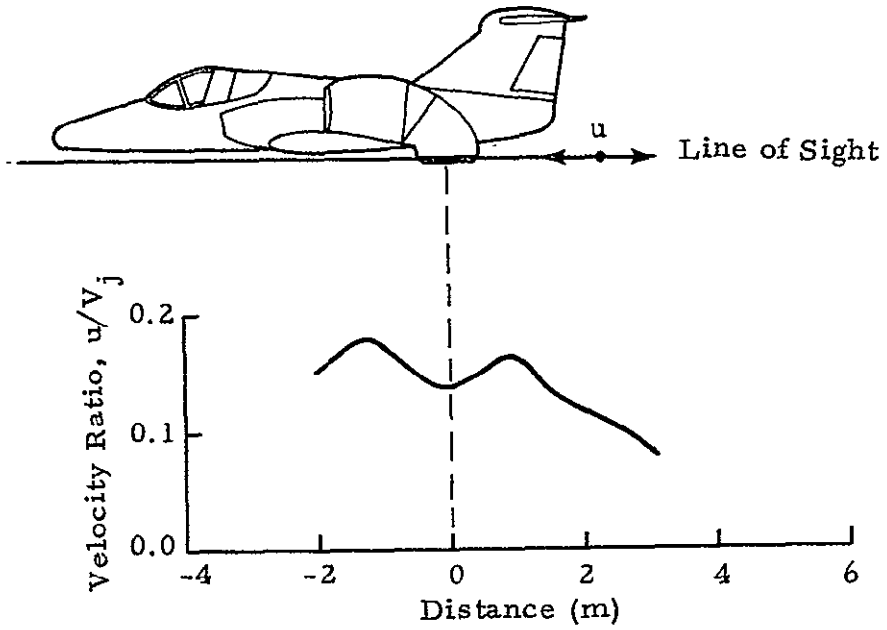

Fig. 28 - Distribution of Horizontal Velocity Along Aircraft Centerline on Bottom of Fuselage

5. CONCLUSIONS AND RECOMMENDATIONS

The present study has shown the following results:

1. Measurements were obtained of the flow around a three-fan 0.7 scale V/STOL aircraft model during static tests and following trends were noted:

   a. Wall Jet — Maximum horizontal velocity is 85% of the jet exhaust velocity and occurs at 1 to 2 diameters from jet centerline at 0.2 to 0.5 diameters above ground.

   b. Fan Jet — Vertical velocity measured by the LDV at the nozzle exit is 80 to 100% of the jet exhaust velocity measured by fan mounted pressure probes.

   c. Fountain — Maximum vertical velocity is 40 to 50% of the jet exhaust velocity and occurs near the ground at the centerline between the two lift cruise engines.

   d. Fuselage Flow — Horizontal velocity along aircraft underside ranges from 10 to 20% of the jet exhaust velocity for two-fan operation.

2. The velocity measurements obtained by the LDV have been compared with available velocity measurements based on pressure surveys and show similar trends.

3. The laser Doppler velocimeter is a viable method for measuring the flow velocities around a hovering V/STOL aircraft. For subsequent investigations, the following improvements to the LDV system are recommended:

   a. Add a translator to the system to resolve the plus and minus flow direction along the line of sight.

   b. Add an improved signal processor to the system to increase the sampling rate to enable measurements of turbulence parameters.

   c. Modify the test pad to accommodate the LDV system and allow three-dimensional scanning with the existing hardware.

   d. Investigate the use of additional LDVs to obtain simultaneous measurements along additional lines of sight to resolve the three components of velocity.

e. Establish the calibration of the LDV by comparison with other proven methods of measuring flow velocity.

f. Determine the effect of the remote mirror assembly on the flow field.

REFERENCES

1. Bower, W. W., "Compressible Viscous Flow Fields and Airframe Forces Induced by Two-Dimensional Lift Jets in Ground Effect," ONR-CR 215-246-2, Office of Naval Research, Arlington, Va., 1 March 1978.
2. Siclari, M. J., P. Aidala, F. Wohllebe and J. L. Palcza, "Development of Prediction Techniques for Multi-Jet Thermal Ground Flow Field and Fountain Formation," AIAA Paper 77-616, Palo Alto, Calif., 6-8 June 1977.
3. Kotansky, D. R., N. A. Durango, D. R. Bristow and P. W. Saunders, "Multi-Jet Induced Forces and Moments on VTOL Aircraft Hovering In and Out of Ground Effect," NADC-77-229-30, June 1977.
4. Behnert, R., and R. Weinraub, "USN/FMOD FRG VAK-191B Joint Flight Test Program — Final Report — Volume 7, "Footprint and Reingestion," NAVAIR-7R-76, August 1976.
5. Lawrence, T. R., D. J. Wilson, C. E. Craven, I. P. Jones, R. M. Huffaker and J. A. L. Thompson, "A Laser Velocimeter for Remote Wind Sensing," Rev. Sci. Inst., Vol. 43, No. 3, March 1972, pp. 512-517.
6. Brashears, M. R., T. R. Lawrence and A. D. Zalay, "Mobile Laser Doppler System Check Out and Calibration," FAA-RD-77-48, June 1977.
7. Schuster, E. P., and J. D. Flood, "Important Simulation Parameters for the Experimental Testing of Propulsion Induced Lift Effects," AIAA Paper 78-1078, Las Vegas, Nev., July 1978.
8. "Static Test Stand Balance Measurements of a Large Scale Model of a Lift/Cruise Fan V/STOL Aircraft," NASA CR to be published June 1979.
9. "Infrared Measurements of a Large Scale Model of a Lift/Cruise Fan V/STOL Aircraft," U.S. Navy report to be published June 1979.
10. Gambucci, B. J., K. Aoyagi and L. S. Rolls, "Wind Tunnel Investigation of a Large-Scale Model of a Lift/Cruise Fan V/STOL Aircraft," NASA TM X-73139, May 1976.
11. Tani, I., and Y. Komatsu, "Impingement of a Round Jet on a Flat Surface," Applied Mechanics Proceedings, 11th Int. Congress, Munich, August 1964, H. Görther, ed., Springer-Verlag, 1966, pp. 672-676.
12. Hrycak, P., D. T. Lee, J. W. Gauntner and J. N. Livingood, "Experimental Flow Characteristics of a Single Turbulent Jet Impinging on a Flat Plate," NASA TN D-5690, March 1970.

Appendix A

DESCRIPTION OF LASER DOPPLER VELOCIMETER SYSTEM

Appendix A

The LDV system developed and fabricated at Lockheed-Huntsville was used to obtain the measurements of the V/STOL flow field during the Ames tests. A description of the LDV system is given, including the principle of operation, the basic optical system and the optic scanning system and the data processing system. The overall system configuration is shown in Fig. A-1.

A.1 PRINCIPLE OF OPERATION

An analogy can be drawn between an LDV and a conventional microwave Doppler radar. The microwave Doppler radar employs relatively long wavelengths of electromagnetic energy which are backscattered by large objects such as aircraft, thunderheads, etc. The LDV transmits much shorter wavelength (10.6 μm) radiation and receives energy backscattered from small objects such as aerosols, water droplets, salt spray, etc. In both cases the velocities of backscattering targets are determined from the Doppler shift of the returned radiation. In the case of the microwave radar, the range of the target is typically determined by round trip time of a pulse of energy from the transmitter to the target and back to the receiver. With the Lockheed LDV depicted herein, the range to the target is determined by focusing the system optics to selectively view radiation backscattered from specified ranges.

An LDV system senses air movement by measurement of the Doppler frequency shift of laser radiation backscattered by the atmospheric aerosol. An instrument must incorporate means to transmit the laser radiation to the region of interest, collect the radiation scattered from the atmospheric aerosol and to photomix the scattered radiation and a portion of the transmitted beam on a photodetector. The difference between the transmitted frequency

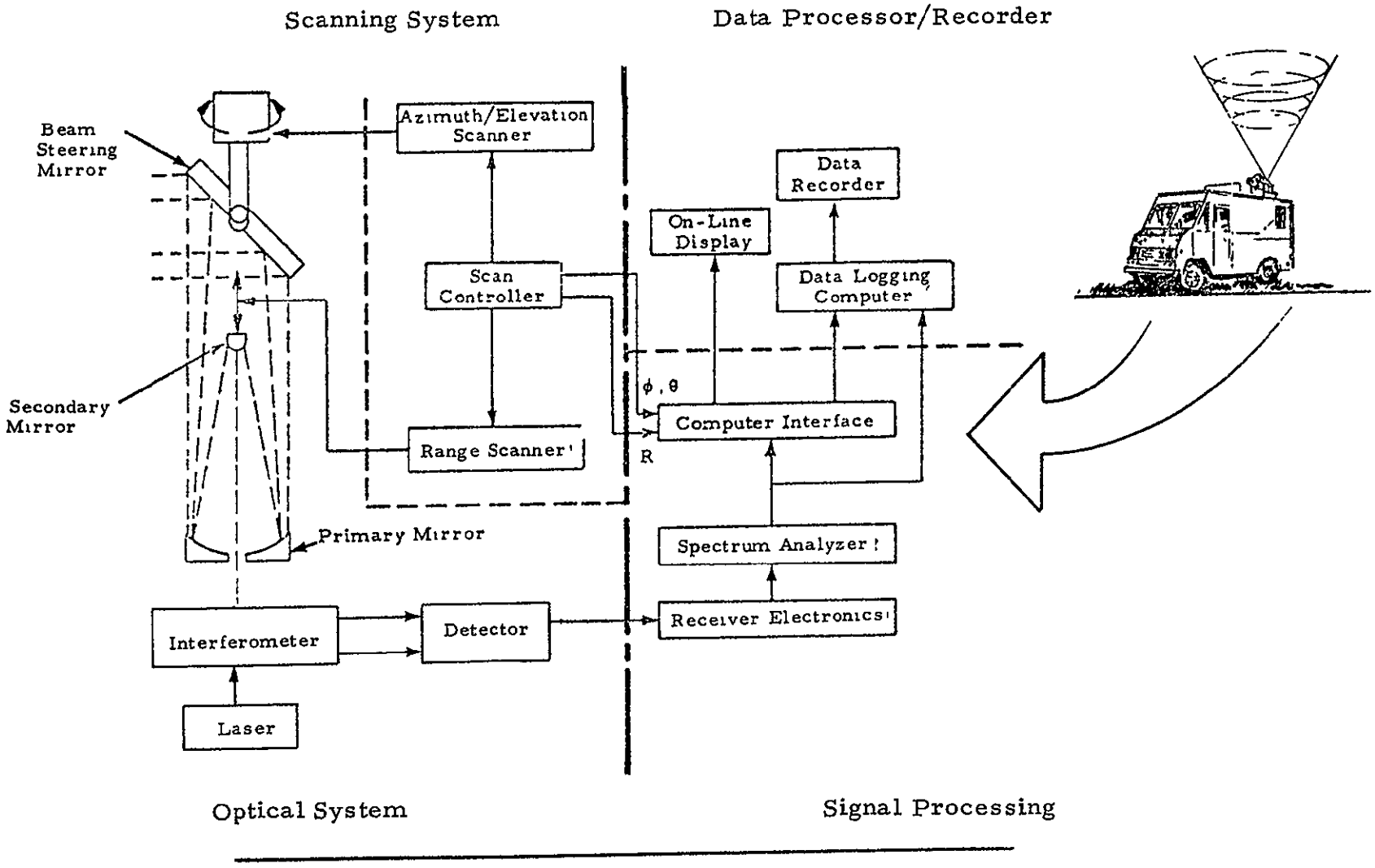

Fig. A-1 - System Configuration

and the returned frequency is the Doppler shift frequency. The Doppler frequency shift signal is generated at the photodetector and is translatable into an analog-optic axis wind velocity component using appropriate electronics. The magnitude of the Doppler shift, Δf, is given by the equation shown below.

$$\Delta f = \frac{2}{\lambda} |\overline{V}| \cos\theta \tag{A.1}$$

where

$\overline{V}$ = the velocity vector in the region being sensed

λ = the laser radiation wavelength, and

θ = the angle subtended by the velocity vector and the optic system line of sight

A Doppler shift of 188 MHz results per m/sec of line-of-sight velocity component. Thus, measurement of the Doppler shift frequency, Δf, yields directly the line-of-sight velocity component $|\overline{V}| \cos\theta$. Some typical advantages of the laser Doppler method are: (1) the Doppler shift is a direct absolute measure of the velocity (for example, the hot wire yields velocity via a cooling effect on the wire); (2) the ease with which the position of the sensing volume can be varied (optics pointing and focusing operations only being involved); (3) the ambient aerosol provides sufficient scattering, thus enabling operation in "clear air" conditions; (4) the ambient aerosol tracer has a small inertia and responds quickly to variations in airspeed and is thus a good turbulence indicator; and (5) from the intensity of the backscattered laser radiation the relative particulate concentration can be determined.

A.2 BASIC OPTICAL SYSTEM

The basic optical system is shown in Fig. A-2. The system depends on focusing the transmitter telescope at the location of interest to control the range at which the measurements are taken.

A horizontally polarized, 20-watt, continuous wave CO_2 laser beam (10.6 micron wavelength) emerges from the laser (1) and is deflected 90 degrees by a mirror (3). The approximately 6 mm diameter beam then

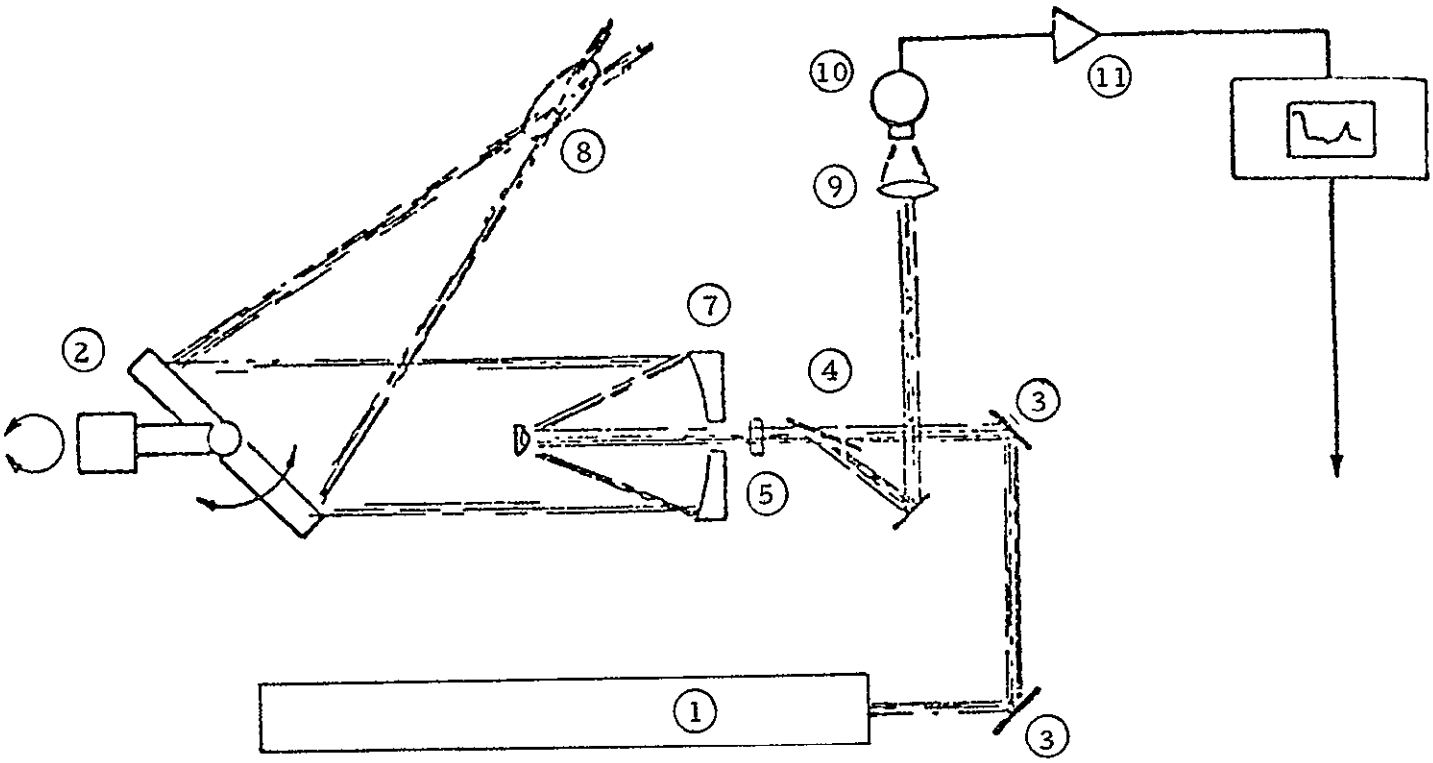

1. CO_2 Laser
2. Mirror
3. Mirror
4. Brewster Window
5. Quarter Wave Plate
6. Secondary Mirror
7. Primary Mirror
8. Focal Volume
9. Lens
10. Photodetector
11. Preamplifier
12. Spectrum Analyzer

Fig. A-2 - Optical Component Configuration of the Lockheed LDV

passes through a Brewster window (4) and a CdS quarter waveplate (5) which converts it to circular polarization. The beam impinges on the secondary mirror (6) and is expanded and reflected into the primary mirror (30 cm diameter) (7) and then focused out into the atmosphere. A small portion of the original laser beam is reflected by the secondary mirror and the Brewster window (4) and is used as a reference frequency on the photodetector (10). Energy scattered by aerosols, at the focal volume (8) is collected by the primary mirror (7), collimated by the secondar (6), and passes through the quarter waveplate (5). The quarter waveplate changes the polarization of the aerosol backscattered radiation from circular to vertical linear polarization. The vertically polarized beam is approximately 78% reflected off the Brewster window (4). After passing through the collecting lens (9) the two beams (i.e., a small portion of the original beam and the beam backscattered from the focal volume) are photomixed on the detector (10) in a heterodyne configuration. The electrical output of the detector (10) is amplified (1) with a 5 MHz bandwidth, 20 dB gain low noise type preamplifier and fed into a spectrum analyzer (12) which gives an output of laser beam intensity as a function of Doppler frequency shift.

A.3 OPTIC SCANNING SYSTEM

To provide the flexibility required to obtain measurements of three-dimensional flows, a scanning arrangement as shown in Fig. A-3 is utilized. The modes of operation include scanning capability in and azimuth and elevation and range. The mirror assembly, AB, can be rotated about the vertical axis for scanning in azimuth. Mirror A is adjusted to control the elevation angle of the beam. The scanning hardware as deployed on the mobile van is shown in Fig. A-4. The system's scan capabilities are shown in Fig. A-5.

Range scanning of the system's focal volume is accomplished by varying the distance between the telescope secondary mirror, E, and the primary mirror, D shown in Fig. A-3. This is effected by varying the position of the secondary mirror, E, in a controlled manner by an electric motor/optical encoder combination. The scan can be conducted through either the overhead scanner or side window.

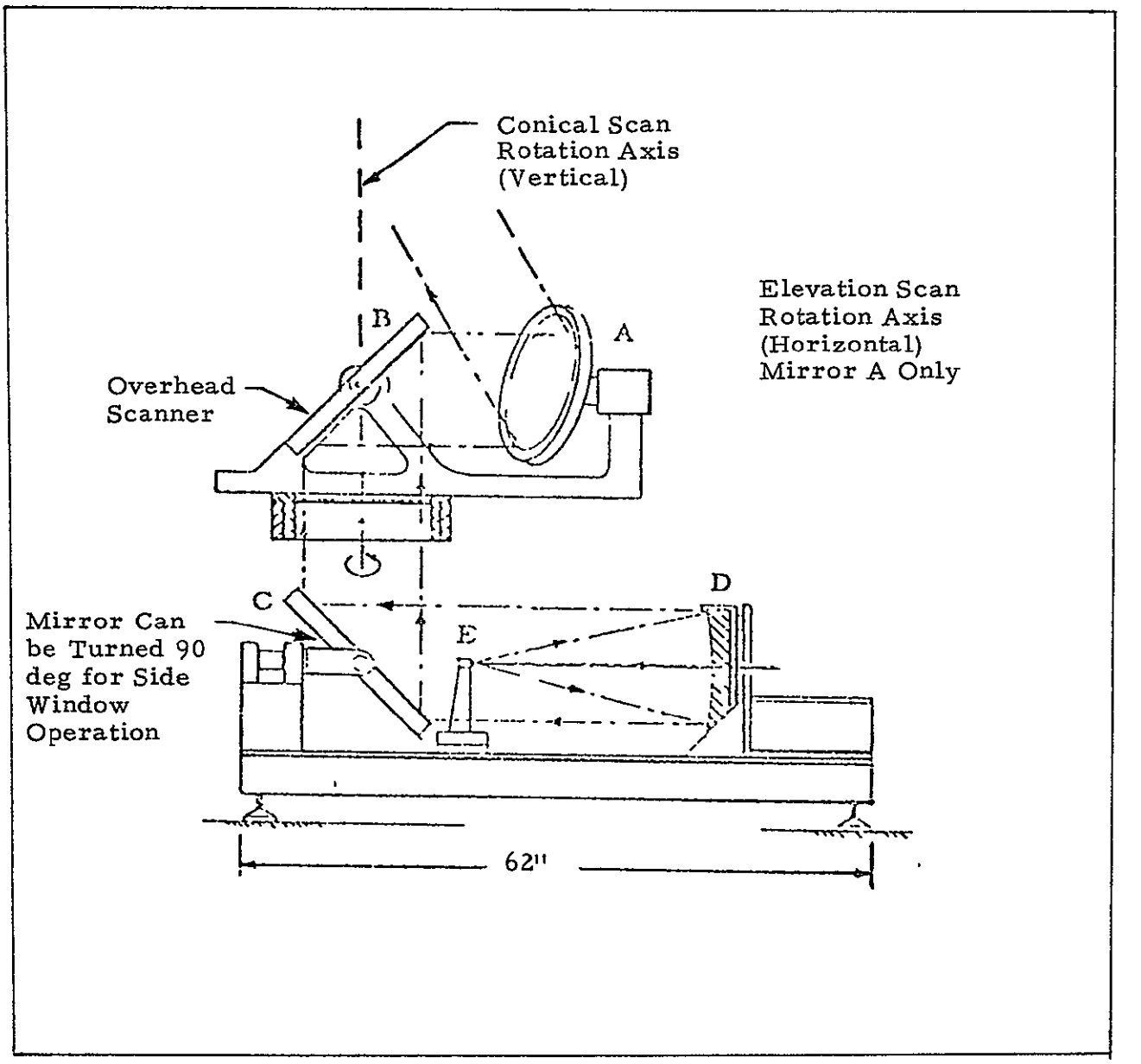

Fig. A-3 - Schematic of LDV Optic Scanning System

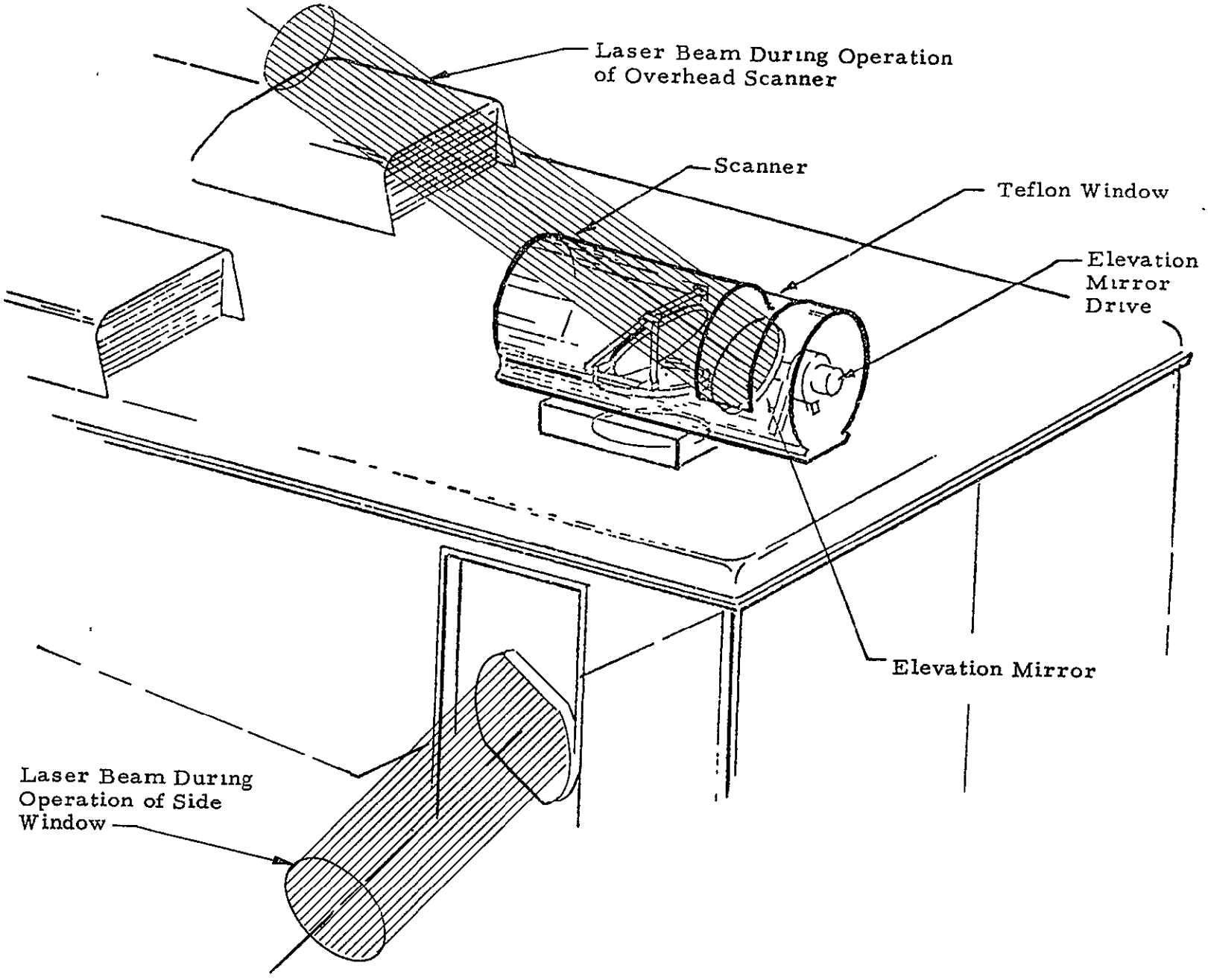

Fig. A-4 - Sketch of Scanning Hardware

BASIC SCAN MODES

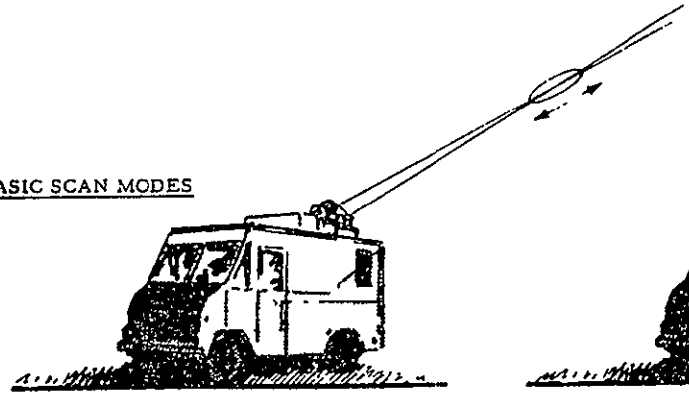

RANGE SCAN

Limits		Rates
Max	Min	
100 to 800 m	16 to 650 m	0 1 to 6 9 Hz
One meter increment		0 1 Hz increm

Also can be stepped between 8 preselected ranges

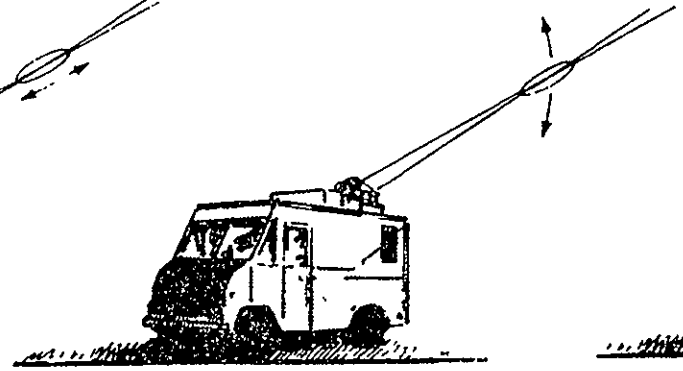

ELEVATION SCAN

	Limits		Rates
	Max	Min	
Scan Center Angle	10 to 90°	0 to 90°	0 1 to 0 5 Hz
Scan Width	90°	10°	
	1 deg increment		0 1 Hz increm

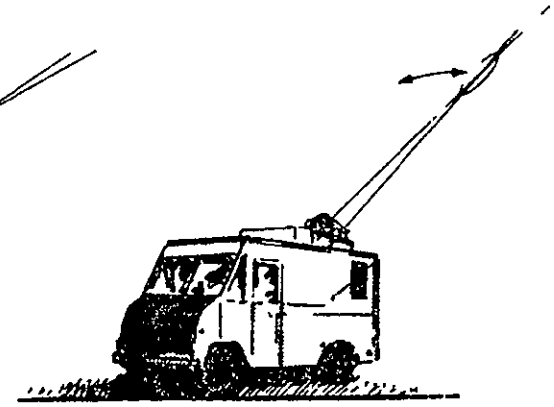

AZIMUTH SCAN

	Limits		Rates
	Max	Min	
Scan Center Angle	300°	0°	15°/sec
Scan Width	90°	10°	
	Open Loop		12 rpm

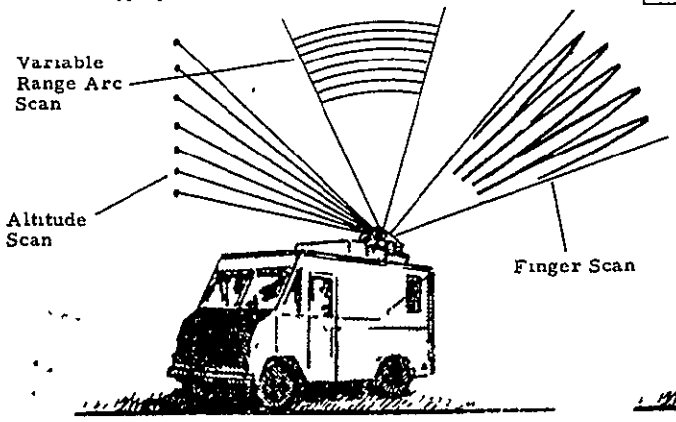

Range - Elevation

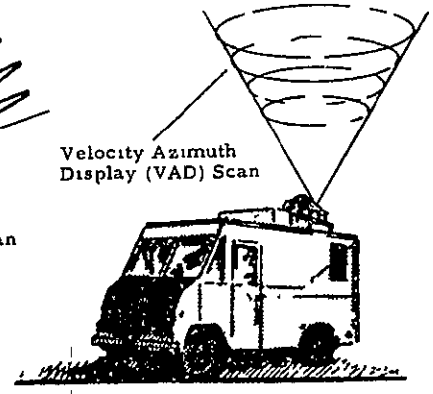

Range - Azimuth

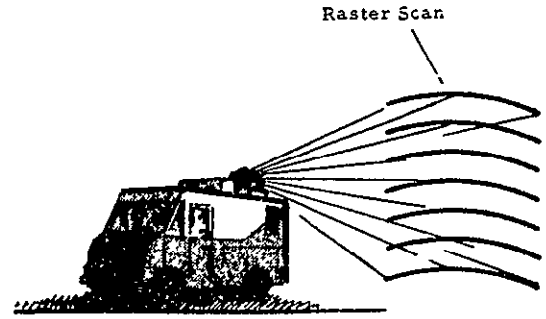

Azimuth - Elevation

Fig. A-5 - Scan Capabilities of Mobile Laser Doppler Velocimeter System

The limits of the focal volume in the range direction are defined as the points at which the intensity of the backscattered radiation per unit depth of the focal volume ishalf of the maximum backscattered intensity per unit depth. For the theoretical distribution of intensity along the focal axis, the sensing volume length, ΔR (i.e., the distance between the two half maximum intensity points) is

$$\Delta R = 4.4\ \lambda R^2/\pi a^2 \tag{A.2}$$

where λ is the laser wavelength (10.6 μm), R is the range to focus, and a is the radius of the telescope primary mirror (15 cm). The theoretical and measured range resolution of the LDV is shown in Fig. A-6. The measured values were obtained by focusing the beam at a hard target for maximum returned intensity and then increasing or decreasing the range until the half maximum intensity points were reached.

The nominal focal volume in the plane normal to the optic line-of-sight axis is defined as the area which contains half of the total laser intensity. The laser intensity in the plane normal to the optic line-of-sight is normally distributed with respect to the transverse direction. The relationship for the lateral limits of the focal volume is

$$\Delta Y = \lambda R/a \tag{A.3}$$

The theoretical and measured transverse spatial resolution of the LDV is tabulated below.

Range to Focus R (m)	Sensing Volume Width ΔY (m)	
	Measured	Eq. (A.3)
50	3.3×10^{-3}	1.8×10^{-3}
100	6.6×10^{-3}	3.5×10^{-3}
200	1.3×10^{-2}	7.0×10^{-3}
600	3.9×10^{-2}	2.1×10^{-2}

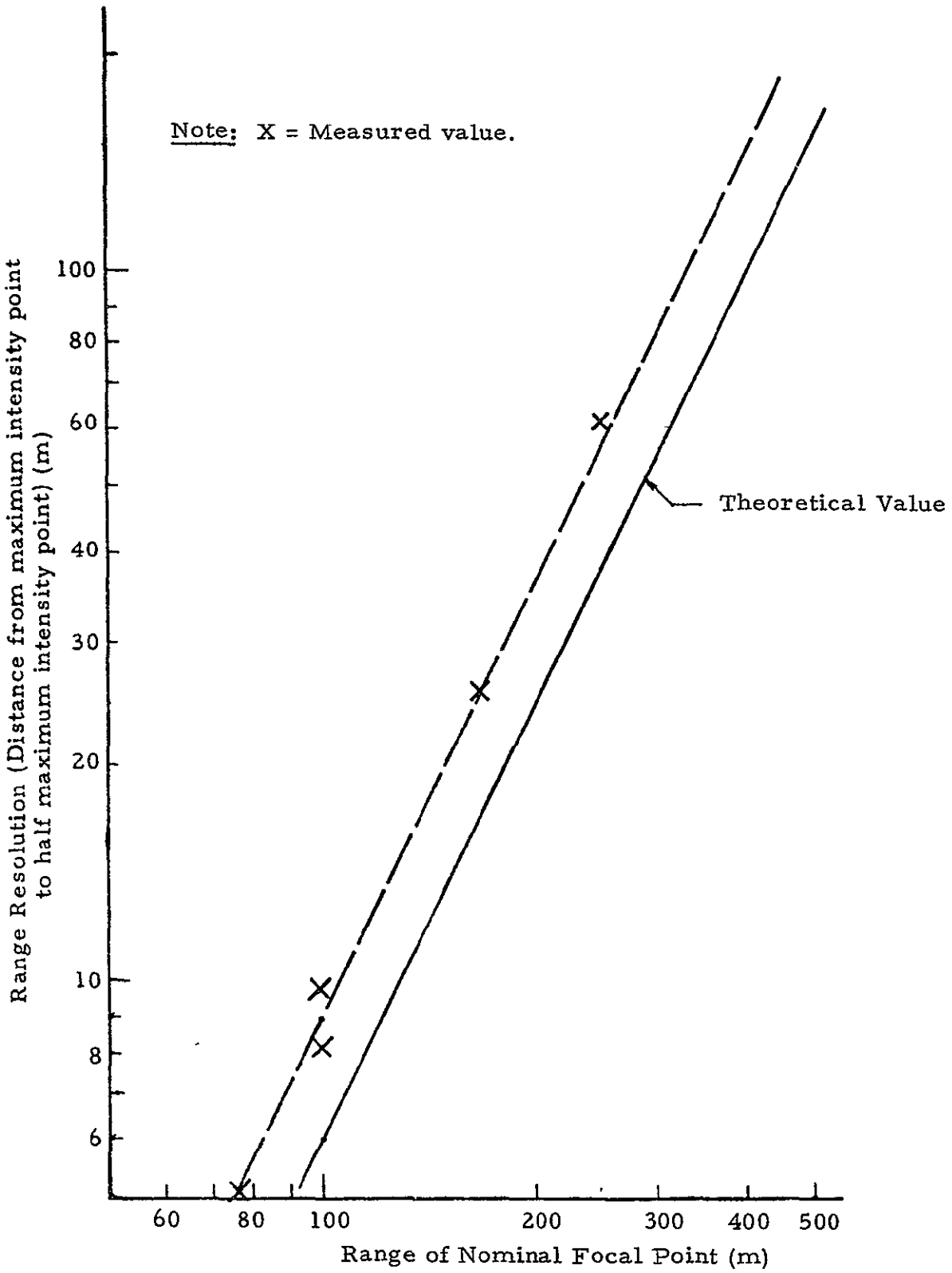

Fig. A-6 - Range Resolution of LDV Measured by Backscattered Intensity

The measured value was obtained from a power meter with a pinhole attachment and is the lateral position at which the power meter reading was e^{-2} of the maximum power meter reading.

The sampling volume of the LDV is a narrow elongated region whose width is small in comparison to the dimensions of the V/STOL flow field but whose length can be some fraction of the spatial dimension of the flow. For example, if the LDV system is measuring the decay of the V/STOL wall jet at a range of 24 m, the half-power level signal is confined to a region ± 0.4 m in length and 0.2 cm in diameter. Assuming the characteristic length scale of the flow is the jet diameter, $D \sim 1$ m, the spatial resolution of the measurement is $\pm 40\%$ of the jet diameter along the line of sight.

A.4 DESCRIPTION OF LDV DATA PROCESSING SYSTEM

Acquisition and processing of the LDV signature is accomplished by means of a compact data handling system developed specifically for the Lockheed-Huntsville mobile LDV. The general elements of the data acquisition and data processing system are shown in Fig. A-7. The digitized LDV intensity versus frequency signal along with its coordinates in space is fed into the PDP 11/34 minicomputer. The minicomputer also has the capability for replaying the data from the 9-track tape and carrying out: (1) detailed processing of the LDV data; (2) generating plots of the processed data on the CRT; and (3) producing hard copy plots and printouts of the processed data.

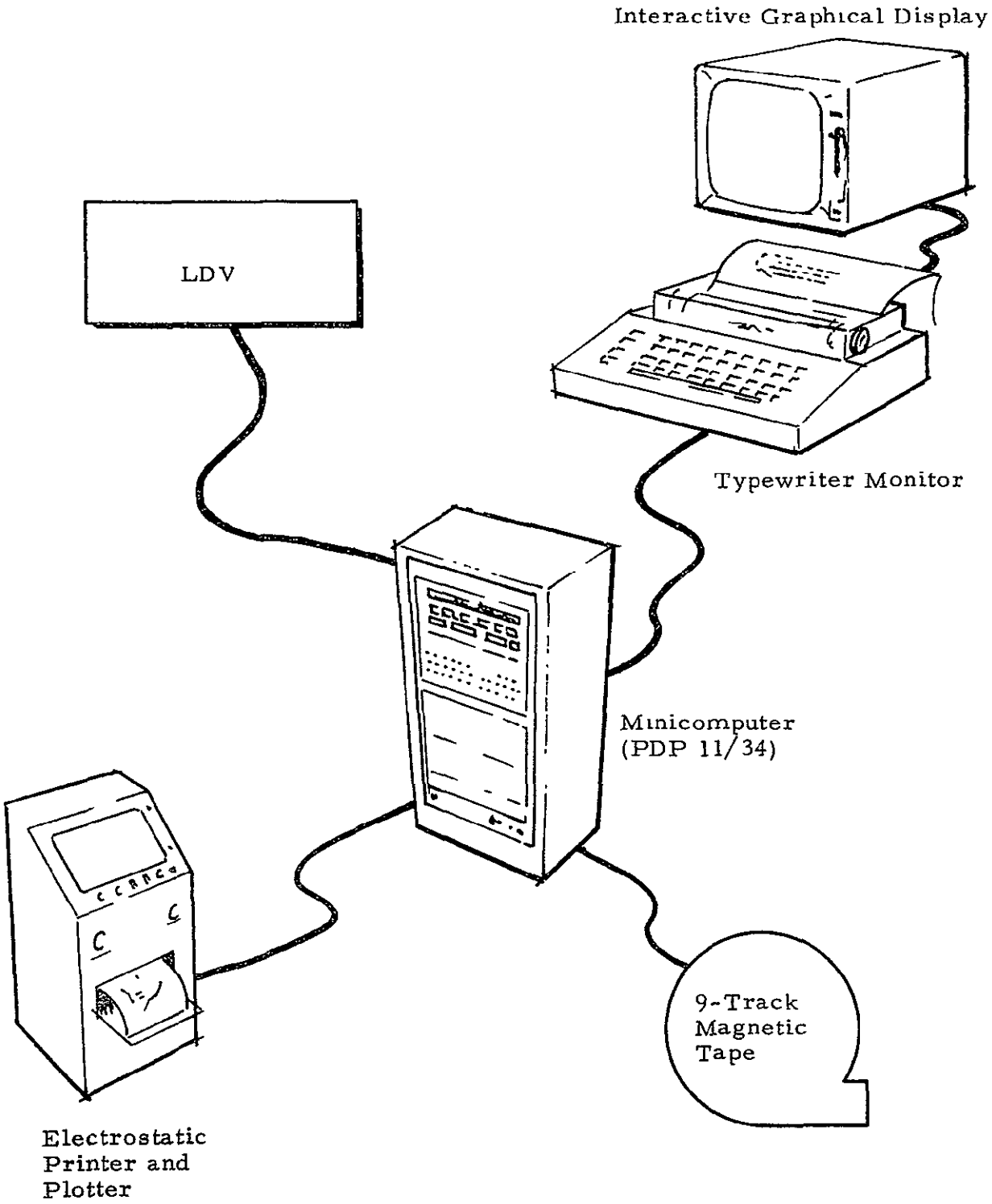

Fig. A-7 - General Elements of LDV Data Acquisition and Data Processing System

Appendix B

SUMMARY OF VELOCITY MEASUREMENTS OBTAINED WITH LASER DOPPLER VELOCIMETER

Selected plots of the line-of-sight velocity versus range are presented in this appendix. From a survey of all of the data, those plots have been selected which are relatively free from noise (i.e., the velocity trends are evident by eye). The line-of-sight velocity is computed from the highest intensity signal (labeled max VPEAK) or from the integrated spectrum (labeled IPV). The plots of VPEAK vs RANGE and IPV vs RANGE were generated by the VTAVQQ and ANDKEN programs discussed earlier in Section 2. The velocity is given in units of COUNTS. The scale factor is 1 COUNT = 1/100 x 20 MHz Doppler frequency shift = 1.06 m/s for all runs with the following exceptions; 1 COUNT = 0.53 m/s for tape Ames 9 Files 4-9 and 19-27; 1 COUNT = 0.26 m/s for tape Ames 9 File 18. The RANGE is measured from the side window of the LDV van to the aircraft. The centerline of the nose fan and lift cruise fan are located at 21 and 28 m RANGE, respectively.